Journal of Hydrology 391 (2010) 157–174

Contents lists available at ScienceDirect

Journal of Hydrology

journal homepage: www.elsevier.com/locate/jhydrol

Roles of the combined irrigation, drainage, and storage of the canal network in improving water reuse in the irrigation districts along the lower Yellow River, China

Lei Liu [a,d], Yi Luo [a,*], Chansheng He [a,c], Jianbin Lai [a], Xiubin Li [b]

[a] Yucheng Comprehensive Experimental Station, Key Laboratory of Ecological Network Observation and Modeling, Institute of Geographic Sciences and Natural Resources Research, Chinese Academy of Sciences (CAS), 100101 Beijing, China
[b] Institute of Geographic Sciences and Natural Resources Research, CAS, 100101 Beijing, China
[c] Department of Geography, Western Michigan University, Kalamazoo, MI 49008, USA
[d] Graduate University, CAS, 100049 Beijing, China

ARTICLE INFO

Article history:
Received 7 March 2010
Received in revised form 11 July 2010
Accepted 14 July 2010

This manuscript was handled by G. Syme, Editor-in-Chief

Keywords:
Combined irrigation
Drainage
Storage

SUMMARY

The commonly used irrigation system in the irrigation districts (with a combined irrigation area of 3.334×10^6 ha) along the lower Yellow River of China is canal network. It delivers water from the Yellow River to the fields, collects surface runoff and drainage from cropland, and stores both of them for subsequent irrigation uses. This paper developed a new combined irrigation, drainage, and storage (CIDS) module for the SWAT2000 model, simulated the multiple roles of the CIDS canal system, and estimated its performance in improving water reuse in the irrigation districts under different irrigation and water diversion scenarios.

The simulation results show that the annual evapotranspiration (ET) of the double-cropping winter wheat and summer maize was the highest under the full irrigation scenario (automatic irrigation), and the lowest under the no irrigation scenario. It varied between these two values when different irrigation schedules were adopted. Precipitation could only meet the water requirement of the double-cropping system by 62–96% on an annual basis; that of the winter wheat by 32–36%, summer maize by 92–123%, and cotton by 87–98% on a seasonal basis. Hence, effective irrigation management for winter wheat is critical to ensure high wheat yield in the study area. Runoff generation was closely related to precipitation and influenced by irrigation. The highest and lowest annual runoff accounted for 19% and 11% of the annual precipitation under the full irrigation and no irrigation scenarios, respectively. Nearly 70% of the annual runoff occurred during months of July and August due to the concentrated precipitation in these 2 months.

The CIDS canals play an important role in delivering the diversion water from the Yellow River, intercepting the surface runoff and drainage from cropland (inflow of the CIDS canal) and recharging the shallow aquifer for later use. Roughly 14–26% of the simulated total flow in the CIDS canal system recharged shallow aquifer through canal seepage. The water flowing out of the canal system accounted for approximately 32% of the water in the CIDS canals. The storage capacity of the CIDS canals is negatively correlated to the precipitation. In years with abundant precipitation, the volume of the surface runoff and drainage from the cropland may surpass the storage capacities of the CIDS canals, while in years with less precipitation, partial storage capacity of the CIDS canal may be occupied by the diversion water from the Yellow River. Proper maintenance of the storage capacity of the CIDS has the potential in improving the efficiency of reusing the surface runoff and field drainage for irrigation practices to mitigate the increasing water shortage along the lower Yellow River.

1. Introduction

Irrigation districts along the lower Yellow River are an important production base of grain and cotton of China, encompassing 32 counties in Henan provinces and 48 counties in Shandong province, with a combined irrigation area of 3.334×10^6 ha (Fig. 1). Main crops in the region include winter wheat, summer maize and cotton. Winter wheat is regularly irrigated; summer maize and cotton are less irrigated due to abundance of the monsoon rains. Water from the Yellow River is a main source for irrigation. The annually averaged water withdrawal from the Yellow River

* Corresponding author. Tel./fax: +86 10 6488 8920.
E-mail address: luoyi.cas@gmail.com (Y. Luo).

0022-1694/$ - see front matter © 2010 Elsevier B.V. All rights reserved.
doi:10.1016/j.jhydrol.2010.07.015

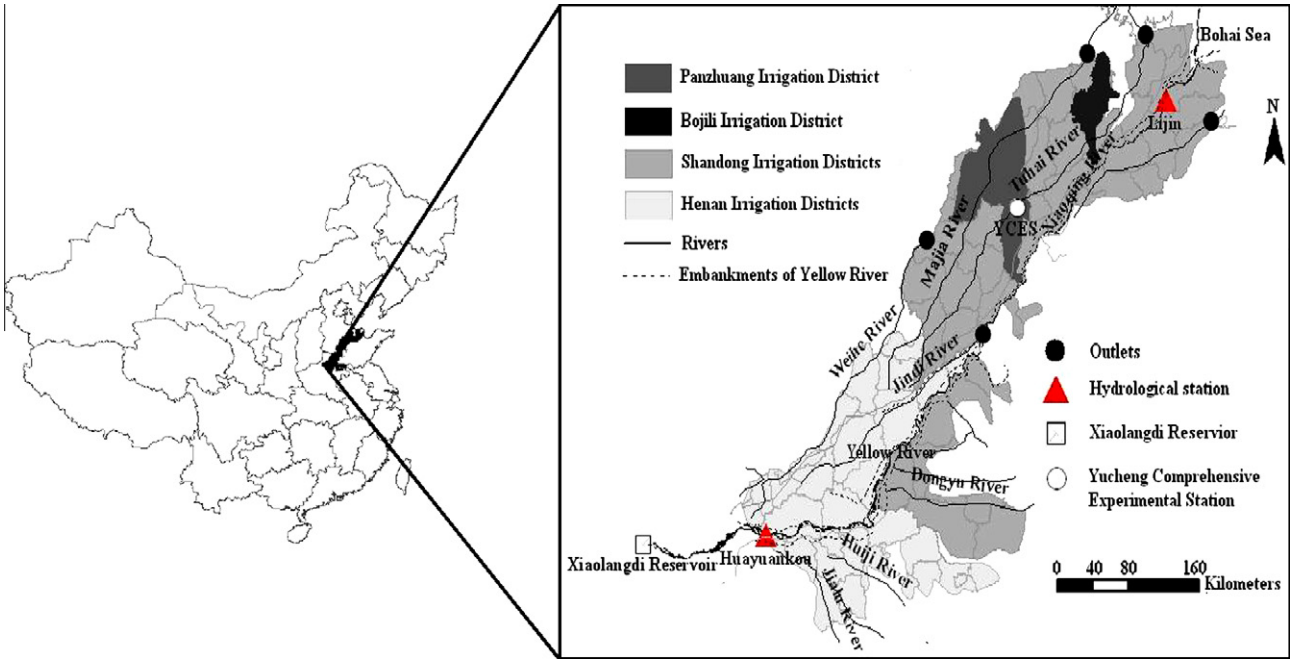

Fig. 1. The study area with major rivers, river outlets, and the location of the Yucheng Comprehensive Experimental Station.

was 8.16×10^9 m^3 from 1985 to 1997 (Yu, 2002), and 8.22×10^9 m^3 from 1969 to 2005 and more than 90% of the diversion was dedicated to irrigation (Hou et al., 2000). However, the irrigation districts are confronting with ever increasing challenge of reducing water supply from the Yellow River because of less river flow, competitions for water from other water users, and water quality deterioration. Meanwhile, underdeveloped irrigation technology and improper irrigation management at both field and regional scales have led to low agricultural water use efficiency. Thus, how to make best use of the limited water resources to guarantee adequate crop production is an urgent issue that needs to be addressed in the study region. The agronomic options of water resources and water use efficiency in the North China Plain were extensively studied and discussed (Fang et al., 2010). However, study on efficiency of the irrigation and water delivery and drainage system, especially at the regional scale, remains quite insufficient.

Canals in the irrigation districts along the lower Yellow River, especially in Shandong province, perform a combined role of irrigation, drainage, and storage (CIDS). Bouarfa et al. (2006) investigated performance of the CIDS canals in Bojili irrigation district (BID) (Fig. 1). The BID, which is located in Shandong province, covers 2.24×10^5 ha and is the most downstream area served by the Yellow River. It diverts about 5.0×10^8 m^3 water annually from the Yellow River to irrigate 1.09×10^5 ha of farmland (Pereira et al., 2003). The CIDS canals can receive runoff, especially after a storm and the runoff can be reused a few days later (Bouarfa et al., 2006). The reuse of drainage waters offers opportunities for improving irrigation water management in areas facing water shortage (Minhas et al., 2006). Bouarfa et al. (2006) quantified the water storage functions of the ditch network system in the BID through analyzing the relationship of rainfall and irrigation recharge, groundwater level fluctuation, and water storage on the basis of observations and remote sensing analysis. However, interactions between surface and groundwater, complicated water transfer processes in the groundwater–soil–plant-atmosphere continuum, and seasonal variation of rainfall and crop water demand make investigating the performance of the CIDS canals in improving water use a challenging issue, especially at a large spatial scale.

Soil Water Assessment Tool (SWAT), a physically-based distributed hydrological model, has been widely used under conditions of different climate, soils, land use and land cover, watershed characteristics, and management practices around the world (Arnold and Allen, 1996; Spruill et al., 2000; Rosenthal and Hoffman, 1999; Chu et al., 2004; Gassman et al., 2007). Efforts have been made to apply the model in agricultural watersheds to simulate plant growth, irrigation management, impact of climate change on irrigation, effects of irrigation on runoff, and interactions among climate, crops, soils, and water (Ritschard et al., 1999; Sophocleous and Perkins, 1999; Gosain et al., 2005; Luo et al., 2008). However, simulating the complicated irrigation canal network of the agricultural watersheds often goes beyond capacities of the current standard version SWAT model. Santhi et al. (2005) developed special modules for the SWAT model to deal with the irrigation canal system. But they only considered canal seepage and surface evaporation loss in the canal water balance. A more comprehensive approach needs to be used to include components of both drainage and surface runoff from the cropland for assessing functions of the CIDS canals in this region.

This paper describes the development of a new module for the SWAT model for simulating hydrology of the CIDS canals at first, and then reports the performance of the improved model in assessing the roles of the CIDS canals in reusing water resources through scenario simulations in the irrigation districts along the lower Yellow River. An innovative feature of the new module is that it considers both surface runoff and drainage in simulating the water balance of the CIDS canals. Thus the simulations have better representation of the irrigation practices in the study region.

2. Materials and methods

2.1. Field experiment

Field experiments of winter wheat and summer maize were undertaken at the Yucheng Comprehensive Experimental Station (YCES) of the Chinese Academy of Sciences, located in the Panzhuang irrigation district (PID) that is one of the irrigation districts within the study area (Fig. 1).

At the experiment site, there are 32 equal-sized plots of $5 \times 10\ m^2$. The 32 plots were constructed in a field of 15 ha and arranged as four parallel rows named A, B, C, and D, with 8 plots in each row numbered sequentially as A1–A8, B1–B8, C1–C8, and D1–D8, respectively. The plots are isolated from each other by concrete barriers of 0.1 m thick, 1 m deep (below ground), and 0.1 m high (above the ground). Soil properties were investigated in plots D1, C3, B5, and A7 from soil samples taken using the auger for every 0.1 m layer. Analysis of the soil texture including bulk density and grain composition was performed in the soil laboratory of the YCES. Neutron probe access tubes were installed in each plot for measurement of soil water content profile. A monitoring well was installed at the site to measure groundwater table. Each plot was irrigated individually through a pipe system and irrigation volume was recorded with hydrometers for each application.

The experimental crops were winter wheat and summer maize, two major crops in the lower reaches of the Yellow River, which were rotated during the period of 2002–2005. The winter wheat is usually planted in early or middle October and harvested in early June of the following year. The summer maize is typically planted in early or middle June and harvested in early October. Details of the winter wheat experiment are given in Luo et al. (2008). The summer maize experiments were carried out with 8 treatments which consisted of four plant densities and two water supply levels: no irrigation and irrigation. Each treatment had four replications. Generally, no irrigation was applied to plots A1–A4, B1–B4, C1–C4, and D1–D4; irrigations were applied to plots A5–A8, B5–B8, C5–C8, and D5–D8. Soil water profiles were measured with neutron probe with 0.1 m incremental depth down to 1.5–2.0 m once a week. Leaf area index (LAI) and biomass of the maize were observed once a week. Three stems were taken randomly from each plot. Leaves from those stems were taken to measure the leaf area with the Li-3100C area meter (Li-COR Biosciences, Lincoln, NE, USA) and the LAI was then calculated for each plant densities. The leaves and stems were oven-dried and weighted to calculate the aboveground biomass per unit area according to the plant density. Daily rainfall, temperature, sunshine hours, and wind speed at 10 m height were recorded at the weather station located at the YCES.

Daily evapotranspiration (ET) was measured by a weighing lysimeter with maize planted in it. The weighing lysimeter has a surface area of $3.14\ m^2$, a rim height 0.1 m, a cylinder soil column height of 5 m below the ground, and weighs roughly 35 tons. Weight of the soil column is recorded through a weighing system with sensitivity of 60 g, measured twice a day at 8:00 am and 8:00 pm, respectively. Water supply to and drainage from the soil column are recorded at the same time. ET from the soil column is calculated by the mass balance approach. Detailed description to the structure, principle, and operation of the weighing lysimeter are presented in Yang et al. (2000, 2007), Luo et al. (2008), and Liu and Luo (2010). The lysimeter ET data are used to evaluate the simulated results of the plots during the model calibration and evaluation.

The experiment data for the winter wheat were used to assess soil water and crop growth modules in SWAT2000, and the soil and winter wheat parameters were obtained from Luo et al. (2008). The data for the summer maize were used to calibrate and evaluate the maize growth parameters in the SWAT2000 model in this paper following the approach of Luo et al. (2008).

The cotton growth parameters in Yang (2005) were used in the SWAT2000 model in this paper. Experiments of cotton growth were undertaken at the YCES from 2003 to 2005. At the experiment site, there are additional 12 plots. The cotton experiments were carried out with three plant densities, and four replications. In the experiments, LAI and biomass of the cotton were observed every 15 days. Three stems were taken randomly from each plot. The measurements of LAI and biomass were done using the same approach as that of summer maize. The cotton growth parameters, such as FRGRW1, LAIMX1, FRGRW2, LAIMX2, and DLAI (Neitsch et al., 2002) were taken from the LAI development curves of cotton in Yang (2005).

2.2. Modeling the combined irrigation, drainage, and storage canals

The SWAT model handles three types of water bodies: reservoirs, ponds/wetlands, and depressions/potholes (Neitsch et al., 2002). A reservoir is an impoundment located on the main channel network of a watershed. Ponds and wetlands are water bodies located within subbasins that received inflow from upstream. In areas of low relief and/or young geologic development, the drainage network may be poorly developed. Watersheds in these areas may have many closed depression areas, referred to as potholes. Runoff generated within these areas flows to the lowest portion of the pothole rather than contributing to flow in the main channel.

In the irrigation districts of the lower Yellow River basin, the canal network delivers water from the Yellow River to fields for irrigation; the ditch network is located within the subbasins, collects both surface runoff and field drainage, and stores water for irrigation use in subsequent applications. When water storage goes over the storage capacity, water overflows into the main channel. Therefore, the ditch network plays a combined role of irrigation, drainage, and storage (Bouarfa et al., 2006). Meanwhile, the CIDS canal network consists of different levels of sub-canals that are commonly trapezoid-shaped. Maintenance of proper water depth within each level of canals is a necessity for guarantying field drainage and salinity control.

The water body functions in the current SWAT model are insufficient to handle the CIDS canal network. The fourth type of water bodies: the CIDS canal was thus defined and modeled in this paper to simulate the combined roles of irrigation, drainage, and storage of the canal network.

2.2.1. Water balance of the CIDS

Daily water balance of the CIDS canal is formulated as:

$$\Delta V = Q_{div} + \beta \times Q_{flwi} - E - SEP - Q_{irr} - Q_{flwo} \quad (1)$$

where Q_{div} is daily diversion water (m^3), Q_{flwi} is daily water flowing into the canal (m^3) which includes surface runoff and drainage from cropland, E is daily surface evaporation of the canal (m^3), SEP is daily seepage of the canal (m^3), Q_{irr} is daily pumping water from the canal for irrigation (m^3), Q_{flwo} is daily overflow out of the canal to the main channel (m^3), and ΔV is daily change of canal water storage (m^3). β is a coefficient that is set as unit 1 in the irrigation districts where the CIDS is implemented and as 0 in the irrigation districts where the CIDS does not exist. Evaporation and seepage of the canal are estimated by:

$$E = \eta \times E_0 \times SA/1000 \quad (2)$$

$$SEP = K_{sat} \times X \times L \times 240/1000 \quad (3)$$

where η is an evaporation coefficient, E_0 is potential evapotranspiration for a given day (mm) and can be computed in SWAT, SA is water surface area of canals (m^2), K_{sat} is effective saturated hydraulic conductivity of canal's bottom (mm/h), and X is wetted perimeter (m), L is length of the canal (m).

Cross sections of the CIDS canals are assumed as trapezoids that are common in the irrigation districts. Assuming that slope coefficient of a canal is m, length of a canal segment is L (m), and width of canal bottom is b (m). When water depth of a canal segment is h, the corresponding water surface area SA (m^2), the wetted perimeter X (m), and the water volume V (m^3), following geometric relationships can be derived simply as:

$$SA = (b + 2mh)L \tag{4}$$

$$X = b + 2h\sqrt{1 + m^2} \tag{5}$$

$$V = (b + mh)hL \tag{6}$$

Define H (m) as the maximum water depth corresponding to the water storage capacity V_m (m^3), then

$$V_m = (b + mH)HL \tag{7}$$

It is common that a complete irrigation system includes three levels of canals, the main, the secondary, and the tertiary ones. The main canals take water from the intake gate of the Yellow River, the secondary canals receive water directly from the main canals and the tertiary canals get water from the secondary canals and deliver water to field.

It is further assumed that the storage capacity of canal system V_m consists of three components, the storage capacities of the main, secondary, and tertiary canals, respectively. Assign:

$$\alpha_i = \frac{V_{m,i}}{V_m} \tag{8}$$

where α_i are ratios of storage capacities of sub-canals to that of the canal system; $V_{m,i}$ is storage capacities of sub-canals; i = 1, 2, 3, represent the main, secondary, and tertiary canals, respectively. Provided that the system storage capacity and the ratios α_1, α_2, and α_3 are known, the system storage capacity can be then split into storage capacities of the main, secondary, and tertiary canals. When the storage capacities of the canals are known, the maximum water depths can be estimated accordingly.

To express *H, h, SA,* and *X* as functions of corresponding water storage volume in canals, assume a ratio of the width to the water depth of the canal λ_i

$$\lambda_i = \frac{b_i}{H_i} \tag{9}$$

where i = 1, 2, 3, representing main, secondary, and tertiary canals, respectively. Under condition of the optimal hydraulic cross-section of the trapezoid, the ratio can be solely expressed by its side-slope ratio m_i (i = 1, 2, 3) (Streeter and Wylie, 1979):

$$\lambda_i = 2(\sqrt{1 + m_i^2} - m_i) \tag{10}$$

The maximum water depth allowed in the canal can be derived from Eqs. (7) and (9):

$$H_i = \sqrt{V_{m,i}/(L_i(\lambda_i + m_i))} \tag{11}$$

where i = 1, 2, 3, represent the main, secondary, and tertiary canals, respectively. For a storage volume V_i (i = 1, 2, 3) in canals, the corresponding water depth h_i (i = 1, 2, 3) can be derived as:

$$h_i = \frac{-\lambda_i H_i L_i + \sqrt{\lambda_i^2 H_i^2 L_i^2 + 4m_i L_i V_i}}{2m_i L_i} \tag{12}$$

The corresponding water surface area and the wetting perimeters can be expressed as:

$$SA_i = \sqrt{\lambda_i^2 H_i^2 L_i^2 + 4m_i L_i V_i} \tag{13}$$

$$X_i = \lambda_i H_i + 2h_i\sqrt{1 + m_i^2} \tag{14}$$

Supposing that the water storage capacity of the CIDS, the allocation ratios among the main, secondary and tertiary canals, and the optimal ratio of water depth to canal bottom width are known, the water surface area and wetting perimeters can be obtained through the above equations, and then the water surface evaporation and canal seepage in Eq. (1) can be estimated.

2.2.2. Routing of the CIDS

The CIDS canal in a subbasin receives and stores water from the Yellow River, and surface runoff and drainage from the hydrologic response units (HRUs) within the subbasin as well. Water stored in the CIDS canal maybe pumped to irrigate crops. When water storage in the CIDS canal exceeds the storage capacity, excessive part goes to the main channel. Seepage from the CIDS canal is assumed to go to the shallow aquifer. Water storage in the CIDS is updated daily. Routing process of the CIDS canal is depicted in Fig. 2, which is a modified version of Fig. 1.5 in the theoretical documentation of SWAT2000 (Neitsch et al., 2002).

Water stored in the CIDS canal is designed as the first source of water supply. When water storage in the CIDS canal of a subbasin cannot meet the irrigation demand of the total HRUs in the same subbasin, the insufficient part can be supplied by other water sources set by the SWAT2000 model, such as reach, shallow aquifer, reservoir and other water sources. If there is not enough water from all the designated sources for irrigation, the irrigation water amount will be adjusted to the water availability or even this application will be cancelled.

2.3. Study area and SWAT model configuration

2.3.1. The study area

The lower reach of the Yellow River runs northeast from the Xiaolangdi Reservoir toward the Bohai Sea with the main stream length of approximately 780 km (Fig. 1). The main stream is constrained between the south and north banks, with its bed elevation higher than the ground elevation. The channel width between the banks ranges from 0.3 to 20.0 km. The channel area within the banks is approximately 2.8×10^4 km^2, where more than 200 million people live adjacent to the Yellow River and on 30.0×10^4 ha of cultivated land. Water is diverted from the Yellow River to irrigate the farmland along the stream banks. The study area covers the irrigation land both within and outside the banks (Fig. 1). It lies between latitude 34°12′ and 38°02′N and longitude 113°24′ and 118°59′E and administratively, encompasses 80 counties of Henan and Shandong provinces in China with an area of 664.6×10^4 ha, of which is 333.4×10^4 ha of irrigation area.

The study area is divided into three parts by the banks of the Yellow River. The Southern part belongs to the Huai River basin, and the northern part the Hai River basin, and the middle part the Yellow River basin. In the northern part, there are four main rivers: the Tuhai, Majia, Wei, and Jindi, all are in parallel to the main stream of the Yellow River and flow into the Bohai Sea. In the southern part, the Wo and Huiji Rivers flow into the Huai River and then to the sea. In the middle part, the Tianran-Wenyan River flows into the main stream of the Yellow River.

Statistical analysis based on daily meteorological data from 1961 to 2005 of 58 national-level stations located within the study area indicates that the averaged annual precipitation was 600 mm with 70% falling during June to September and 30% during the winter wheat growth season; the averaged annual temperature was 13.5 °C.

2.3.2. The SWAT2000 model configuration

Ground elevation of the study area decreases gradually along the main stream of the Yellow River from 90 m in the upper reach to a few meters in the lower reach with slope varying between 1/6000 and 1/10,000. The existing DEM resolution is too coarse to distinguish the detailed topographic features. The densely distributed irrigation and drainage canal networks and the tributaries make automatic delineation of subbasins a difficult task to fulfill.

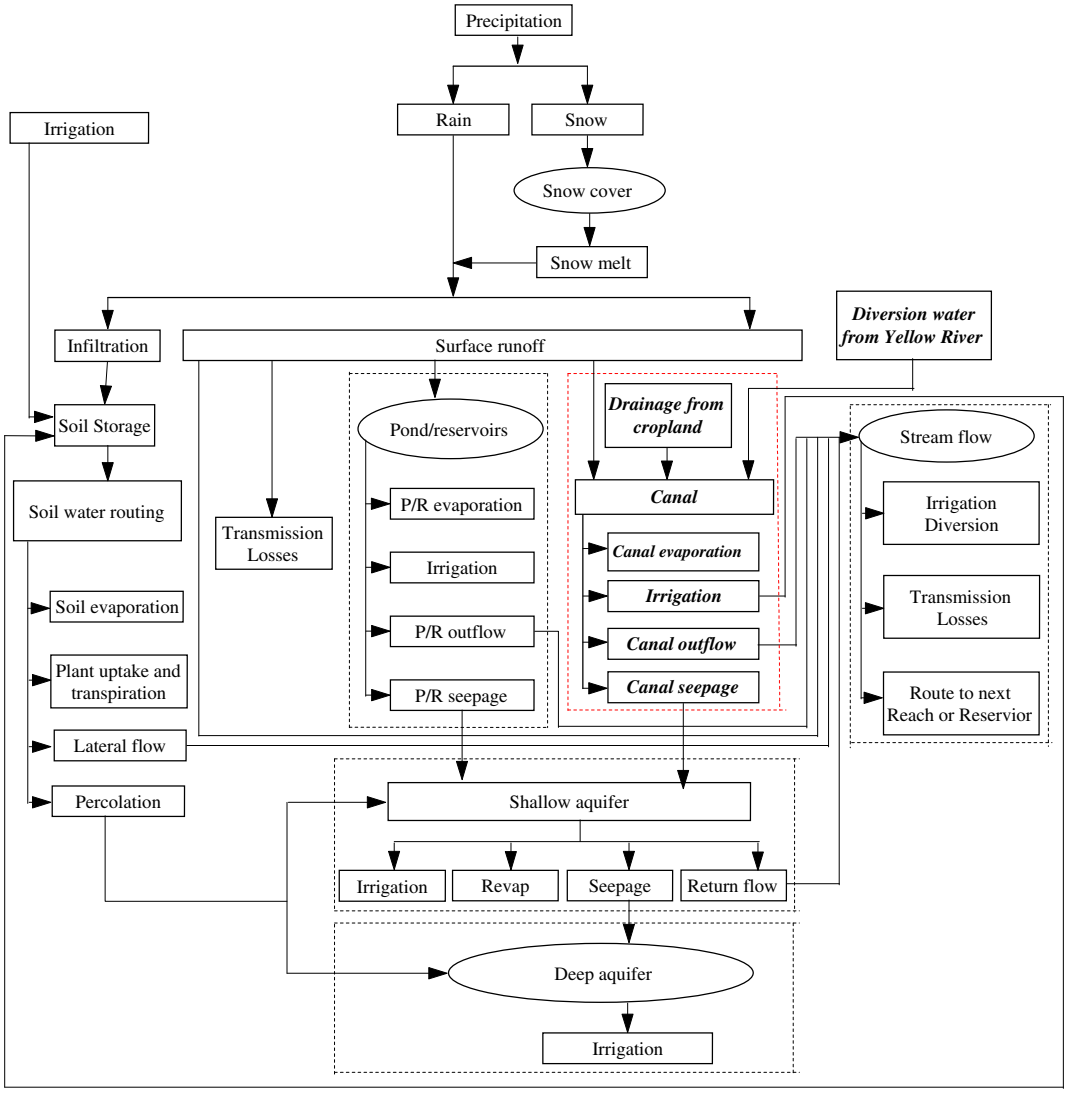

Fig. 2. Water balance schemes in the combined irrigation, drainage, and storage (CIDS) canal irrigation system (the bold Italic parts).

Hence, delineation of subbasins in the study area is performed manually instead of automatically due to the flat topography. Basically, counties are both the administrative units and the water management units in the study area. Therefore, the manual delineation of the subbasins was performed with combined considerations of the natural river network, the artificial canal network, and the basic water management units. Consequently, the study area is divided into 80 subbasins.

There are quite a few outlets for streams flowing out of the study area due to the flat topography. The multiple outlets are simplified as five outlets eventually for rivers flowing out of the study area: the Tuhai River, Majia River, Wei River, Jindi River, and Xiaoqing River (Fig. 1). Stream flow within subbasin was manually routed through the rivers. For the subbasin where there are more than one secondary river running through, it is simply assumed that the stream discharges are routed through the longest one within the subbasin.

2.4. Data preparation

2.4.1. Weather

Weather data from 58 national-level meteorological stations were used in the study. The daily meteorological data series from 1961 to 2005 include maximum and minimal temperature (°C), wind speed at 10.0 m height (m/s), relative humidity, precipitation (mm), and sunshine hours (h). Penman–Monteith method (Monteith, 1965; Allen, 1986; Allen et al., 1989) embedded in the SWAT2000 model was used to estimate the daily potential evapotranspiration (Neistch et al., 2002).

2.4.2. Land use and land cover

Land use/cover data of the year 2000 with a scale of 1:100,000 was used in this study (http://www.geodata.cn). The main land cover types include farmland, forest, grass, barren, urban, and water bodies, which account for 80.8%, 0.8%, 1.2%, 1.5%, 13.2% and 2.5% of the study area, respectively. According to the census reports (Henan Rural Social and Economic Survey Team, 2001; Shandong Bureau of Statistics, 2001), main crops in the area include winter wheat, summer maize, cotton, soybean, vegetation and other minor crops. For the SWAT model simulation, cropland was further classified into winter wheat, summer maize, cotton, soybean, vegetation, and minor crops. Eventually, 11 types of land use and land cover, namely the forests, grass, barren, urban, water bodies, winter wheat, summer maize, cotton, soybean, vegetable and other minor crops are presented in the SWAT model simulation. The planting area of winter wheat, summer maize and cotton

accounted for 37.4%, 18.6% and 8.4% of total planting area in 2000, respectively.

2.4.3. Soils

Soil map of 1:1,000,000 was used in this study (http://www.geodata.cn). Sand, loam, and clay soils account for 25.6%, 67.8% and 6.6% of the area, respectively. The soil profile properties are needed as input to the SWAT model. Approximately 115 soil profiles were investigated over the study area to determine the soil profile properties. The investigation sites were determined on the basis of the spatial distribution of soil types and evenly distributed over the entire study area. Consequently, there are 1 or 2 profiles within a subbasin. The soil profiles were dug to 2 m below the ground at 0.2 m increment using hand-held augers. Grain analysis was done in the laboratory at the YCES for the soil samples using the methods of sieving and hydrometer. Soil bulk densities were obtained using rings of 50 cm^3 in volume through weighing method. The SWAT model estimates soil wilting point based on the clay content and bulk density. In the soil sampling sites, the saturated hydraulic conductivity was measured by Model 2800K1 Guelph Permeameter. Available water capacity was calculated by soil texture triangle hydraulic properties calculator (http://weather.nmsu.edu/Teaching_Material/soil456/soilwater.html). For soil types without the investigated profiles, the nearest neighboring soil profiles of similar soil types were used to infer the soil properties instead.

2.4.4. Hydrologic response units

Heterogeneities exist within a subbasin with respect to soil and land use and land cover. To resolve these heterogeneities, a practical alternative is to represent the effects of these heterogeneities statistically by use of the hydrologic response unit (HRU) (Leavesley et al., 1983). HRUs are lumped land areas within the subbasin that are comprised of unique land cover, soil, and management combinations (Neitsch et al., 2002). The approach can provide considerable spatial detail on large basins without simulating each individual field (Sophocleous and Perkins, 2000). The spatial weight for each HRU can be given by the product of the areal fractions of its defining soil type and land use (Perkins and Sophocleous, 2000) or by overlaying the land cover types and the mapped soil types in spatial data processing tools such as ArcGIS. In this study, HRUs were first generated with the aid of ArcGIS 9.1. Then, HRUs of 'cropland' type were split into different 'crop types', winter wheat, summer maize, cotton, soybean, vegetable, and minor crops, according to the percentage of each crop's planting area within each subbasin outside ArcGIS 9.1 (Henan Rural Social and Economic Survey Team, 2001; Shandong Bureau of Statistics, 2001). A total of 1642 HRUs were generated in the study area, averaging approximately 21 HRUs per subbasin, with a range of 8–30 HRUs per subbasin.

2.4.5. Agricultural management

Agricultural practices, such as sowing, harvests, and irrigation schedules were based on observational data at the YCES and field surveys (interviews and questionnaires with the farmers) carried out around the irrigation districts. In this study, restrictions of N and P were not considered.

2.4.5.1. Planting and harvesting. Winter wheat-summer maize is the most popular planting system in this region. Winter wheat–soybean is also adopted although not very common. Cotton becomes main cash crop in some counties, such as Caoxian, Shenxian, Liaocheng, Guanxian and so on in Shandong IDs and in Qixian, Tongxu, Weishi and so on in Henan IDs. The growth season of the wheat is around 240 days and that of summer maize around 110 days. Growth season of the soybean is very similar with that of the summer maize. Cotton is usually planted around the middle of April and harvested around the middle of October.

2.4.5.2. Potential heat units. Potential heat units were estimated for crops using the approach in the theoretical document of SWAT2000 (Neitsch et al., 2002) and the meteorological data at the weather stations around the study area.

2.4.5.3. Irrigation. In 2007 and 2008, we carried out agricultural water use survey across the study area through in situ interviews and questionnaires with farmers. Eventually, 158 questionnaires were obtained, among which 149 contained irrigation information for winter wheat, 139 for summer maize, and 68 for cotton. The farmers were asked how many times of irrigation and when the irrigation was usually practiced to crops during the last 5 years. The returned questionnaires cover all the counties in the study area, well representing the common cropping and irrigation practices in the lower Yellow River. A summary of the questionnaires is described below.

Winter wheat is usually irrigated two to four times. About 47% of the interviewed winter wheat planters irrigate winter wheat three times during the whole growth season, 30.9% irrigate two times, and 15.4% irrigate four times. There is no report of no irrigation. Winter wheat is always irrigated but never more than four times according to the survey. Percentages of the interviewed planters who irrigate the winter wheat at the re-greening, stem extension, and grain filling stages reached as high as 97%, 78%, and 53%, respectively. The planters may irrigate the crop at other growth stages such as sowing, winter dormancy, and flowering, however, the percentages is as less as 5–14%. Meanwhile, according to the 'Handbook of Irrigation' of the Ministry of Water Resources of China (1994), three irrigations at re-greening, stem extension, and grain filling stages, respectively, are necessary for winter wheat in Henan and Shandong Province. Additional irrigation at sowing is proposed. However, it is performed not as often as before according to the interviewed winter wheat planters. Research also found that saving the sowing irrigation water for use at the sensitive growth stage may generate higher water use efficiency (Fang et al., 2010). Accordingly, irrigations at re-greening stem extension, and grain filling stages were always taken into account in the simulation; additionally, as a traditional practice although not performed as often as before, irrigation during the winter dormancy period is also considered. The irrigation date varies among years and locations within the study area. For simplification, the winter irrigation was assumed on December 10th; irrigations for re-greening, stem extension, and grain filling were assumed on March 15th, April 15th, and May 15th, respectively, which are around the middle of the growth stages. The famers did not provide sufficient information on water amounts applied for irrigations, and data from field experiment and modeling studies give irrigation quotas varying from 45 to 105 mm for winter wheat (Ministry of Water Resources of China, 1994; Fang et al., 2004; Xiao et al., 2006; Li et al., 2008; and Fang et al., 2009). Thus, 75 mm of water in depth per irrigation was adopted in this study.

Percentages of the interviewed maize planters performing one and two irrigations for the summer maize were 45.3% and 48.9%, respectively. None of them irrigated the summer maize more than two times per season. Those who did not irrigate the maize at all accounted for only 5.8%. Nearly 90% of them irrigated at the sowing stage, and 32% at the emergence stage. Those who performed irrigation at other growth stages were less than 10%. Therefore, irrigation at the sowing stage is necessary and most common. Irrigation quotas were based on the published literatures, which varied from 45 to 105 mm for summer maize (Ministry of Water Resources of China, 1994; Liu et al., 2005; Fang et al., 2009; Shao et al., 2009).

Accordingly, it was simply assumed that the summer maize is irrigated 75 mm on June 12 in this study.

Over 63.5% of the interviewed cotton farmers irrigated cotton only once and 23.5% irrigated twice during the cotton season, and 16.2% of them did not irrigate cotton at all. About 84% of them irrigated cotton at the sowing stage, and those who irrigated cotton at other growth stages took accounted for no more than 10%. Irrigation quotas varied between 45 and 105 mm (Ministry of Water Resources of China, 1994; Wu, 2003; Liu et al., 2005). In this study, irrigation at the cotton sowing stage was assumed on April 15 with 60 mm water and at the bud stage on June 20 with 90 mm water, respectively.

2.4.6. Storage capacity of the CIDS canals

The field survey around the irrigation districts found that natural streams cross the irrigation districts in Shandong province are the primary level of the drainage system and part of the main canals for water delivery as well. Dams and gates are used to control the natural streams in order to store water for irrigation. The artificial secondary canals connect the main and tertiary canals. Due to the flat topographic conditions, the flow of stored water may occur from the secondary to the tertiary canals or vice versa. The tertiary canals deliver water to field, collect surface runoff and drainage from field, and store the water for later use. Bouarfa et al. (2006) determined the density of tertiary ditches for each division of the BID through remote sensing and ground investigation in order to quantify the water storage capacity of the system. The storage capacity of the ditches was assumed a typical cross-section of 10 m^2, which corresponds to the most frequent ditch geometry. Based on the product of the length of the ditches and their cross-section divided by the surface area of the division, the estimated storage capacities for each division vary between 20 and 30 mm. A higher value was obtained for the divisions located upstream due to the greater density of ditches (2.7 km/km^2 upstream against 2.1 km/km^2 downstream). This study assumed that irrigation districts had similar density of tertiary ditches to that of BID given by Bouarfa et al. (2006).

The storage capacity given by Bouarfa et al. (2006) for BID was extended to other irrigation districts in Shandong. Further, the storage capacity of the tertiary canals was assumed to account for 60% of the total capacity of the CIDS canal system, and the storage capacities of the secondary and the main canals account for 30% and 10% of storage capacity of the CIDS canal system, respectively.

2.4.7. Records of the water diversion from the Yellow River

Water diversion data from the Yellow River from 1961 to 2005 were collected from the Irrigation Management Bureaus of Henan and Shandong Provinces (Department of Water Resources of Henan Province, 1985–1992; Department of Water Resources of Shandong Province, 1985–1992) and hydrologic records at the Huayuankou Hydrological Station and Lijin Hydrological Station which are located at the upper most and end part of the study area, respectively (Fig. 1). Part of the diversion data are in annual values, and part of them in monthly values. As daily values are required for the SWAT2000 model input, the annual diversion values were downscaled to monthly values following the monthly distribution pattern of diversion records from 1961 to 2005. The monthly diversion water was delivered to the subbasins according to the daily irrigation requirements. It was assumed that the monthly diversion water was only for the current monthly diversion water use. If the monthly diversion water was larger than the actual water use, the surplus water was assumed directly flowing into main channels; otherwise, the insufficient water was diverted from other water sources, such as shallow aquifer storage, reach and so on.

2.5. Calibration and evaluation

In some cases especially in agricultural watershed, groundwater levels, ET, irrigation efficiency and canal conveyance efficiency, etc. have been used to calibrate distributed hydrological models (Querner et al., 1997; Santhi et al., 2005) instead of stream flow data. In this study, parameterization of the SWAT2000 model is based on the data set at the field scale due to the limited data availability in the large study area. The plant growth parameters in the SWAT model include mainly the radiation use efficiency, the harvest index and the six parameters for determining shape of the LAI curve for optimal conditions, the maximum canopy height, maximum root depth, optimal and base temperatures for plant growth, etc. (Neitsch et al., 2002). These parameters of winter wheat and summer maize were calibrated and evaluated with the field experiment data. Luo et al. (2008) assessed the soil and crop growth modules of the SWAT2000 model using the field experiment data of winter wheat, and obtained the soil and winter wheat growth parameters. In this study, summer maize data obtained at the same site were used to calibrate and evaluate the maize growth parameters following the approach of Luo et al. (2008). LAI curve parameters for cotton were derived from the development process of LAI and biomass of cotton from the experimental work by Yang (2005). Growth parameters for soybean were determined by adjusting the default values in the SWAT2000 model (Neitsch et al., 2002) using the LAI and biomass curves in the study of Zhang et al. (2006). The calibrated and evaluated crop parameters were then extended to the whole study area. It should be noted that while the cultivars of winter wheat, summer maize, and cotton and the relevant growth parameters used in the simulations represent the commonly planted crop cultivars in the study region based on the irrigation survey, uncertainties that might be caused from up-scaling the crop parameters from plot scale to the study area was not discussed in this paper due to data insufficiency.

Nash–Sutcliffe efficiency (*NSE*), the ratio of the root mean square error to the standard deviation of measured data (*RSR*), and coefficient of determination (R^2) were used to evaluate the model performance as "very good", "good", "satisfactory" and "unsatisfactory" (Moriasi et al., 2007).

2.6. Simulation scenarios

Thirteen scenarios are designed to investigate how the irrigation applications and water sources influence the performance of the CIDS canals in improving long term water use efficiency. Daily meteorological data series from 1961 to 2005 were obtained from 58 national-level weather stations within the study area. The scenarios are combinations of crop irrigation options and irrigation water sources (Table 1). Three irrigation options were adopted in the study, automatic irrigation, scheduled irrigation, and no irrigation. For the automatic irrigation option, a soil water stress threshold value and crop water stress threshold value were predefined. The crop water stress index is defined to check if the crop is growing or not. When soil water stress is higher than the threshold value and the crop is growing, irrigation is triggered automatically. The soil water threshold value is defined as 80% of the field capacity of the soils (Zhu et al., 1991; Zhang et al., 2002, 2009; and Ren et al., 2003). In this study, it was assumed that once the soil water storage in the top 0.6 m soil layer was depleted to 80% of the field capacity, irrigation was triggered. The automatic irrigation option and none irrigation option are assumed as the two extremes of the irrigation water use. The scheduled irrigation options are basically derived from the in situ questionnaires with the farmers, the 'Hand Book' of the Ministry of Water Resources of China, and publications of field experiments and modeling studies of irrigation.

Table 1
Irrigation scenarios of different irrigation schedules and irrigation water sources.

Scenarios	Irrigation schedules and amount							Irrigation water sources
	Winter wheat				Summer maize	Cotton		
	10-December	15-March	15-April	15-May	12-June	15-April	20-June	
1				Auto				CW or GW
2	75	75	75	75	75	60	90	CW or GW
3	75	75	75	75		60	90	CW or GW
4		75	75	75	75	60	90	CW or GW
5		75	75	75		60	90	CW or GW
6		75	75	75	75	60		CW or GW
7				None				No
8				Auto				GW
9	75	75	75	75	75	60	90	GW
10	75	75	75	75		60	90	GW
11		75	75	75	75	60	90	GW
12		75	75	75		60	90	GW
13		75	75	75	75	60		GW

Note: Auto: auto irrigation option which irrigation is triggered by a threshold value of soil water content and checked with the threshold value of crop water stress; No: no irrigation; CW, canal water; GW: ground water.

For the winter wheat, irrigation at greening, stemming, and grain filling stages are always applied. Winter irrigation, as a traditional management practice, is taken into account as well. For the summer maize, only the irrigation at sowing stage is considered. For the cotton, Irrigation at the sowing stage is always adopted. Additionally, irrigation at the bud stage is also taken into account.

3. Results and analysis

3.1. Calibration and evaluation

3.1.1. LAI and biomass

Table 2 shows indices of NSE, RSR, and R^2 for evaluating the simulated values of LAI and biomass for 32 plots for the year 2004 and 2005. For either LAI or biomass, all the indices indicated very good agreement between the simulated and the measured values for both years. For stage-2, the simulated LAI was mostly rated as "unsatisfactory" in 2004; however, the performance showed mostly good agreement in 2005. This might be due to the inter-seasonal variability of crop parameters of the generic crop growth module (Luo et al., 2008) of the SWAT model. Similarly, the performance of biomass simulations was improved quite a lot in 2005, and this might be either due to the inter-seasonal variability of the growth parameters (Luo et al., 2008), or implying that the leaf senescence approach in the growth module of the SWAT model still has room to improve. For the whole growth period in 2004 and 2005, all the indices, NSE, RSR, and R^2, for either LAI or biomass indicated that the model performance is "very good" in most cases, with the exception of the

Table 2
Statistical indices for assessing performance in 2004 and 2005 with regard to LAI and biomass.

Plots		2004						2005					
		LAI			Biomass			LAI			Biomass		
		Whole stage	Stage-1	Stage-2	Whole stage	Stage-1	Stage-2	Whole stage	Stage-1	Stage-2	Whole stage	Stage-1	Stage-2
A1–A4	R^2	0.92	0.94	0.82	0.97	0.96	0.85	0.95	0.98	0.86	0.99	0.99	0.89
	NSE	0.91(V)	0.92(V)	0.59(S)	0.97(V)	0.86(V)	0.83(V)	0.93(V)	0.96(V)	0.77(V)	0.97(V)	0.94(V)	0.90(V)
	RSR	0.30(V)	0.29(V)	0.64(S)	0.17(V)	0.38(V)	0.42(V)	0.26(V)	0.19(V)	0.48(V)	0.17(V)	0.24(V)	0.32(V)
B1–B4	R^2	0.90	0.92	0.84	0.97	0.96	0.89	0.95	0.98	0.78	0.99	0.99	0.42
	NSE	0.77(V)	0.84(V)	−2.17(U)	0.89(V)	0.84(V)	0.40(U)	0.92(V)	0.94(V)	0.78(V)	0.96(V)	0.96(V)	0.83(V)
	RSR	0.48(V)	0.39(V)	1.78(U)	0.33(V)	0.40(V)	0.77(U)	0.28(V)	0.24(V)	0.47(V)	0.19(V)	0.21(V)	0.41(V)
C1–C4	R^2	0.97	0.99	0.94	0.98	0.97	0.88	0.95	0.97	0.78	0.99	0.99	0.65
	NSE	0.83(V)	0.89(V)	−1.28(U)	0.92(V)	0.80(V)	0.50(S)	0.87(V)	0.89(V)	0.70(S)	0.95(V)	0.92(V)	0.81(V)
	RSR	0.41(V)	0.33(V)	1.51(U)	0.28(V)	0.45(V)	0.70(S)	0.36(V)	0.34(V)	0.55(S)	0.23(V)	0.29(V)	0.44(V)
D1–D4	R^2	0.97	0.99	0.97	0.99	0.96	0.95	0.96	0.99	0.68	0.99	0.99	0.56
	NSE	0.52(S)	0.46(U)	−4.31(U)	0.80(V)	0.43(U)	−0.13(U)	0.49(U)	0.59(S)	−0.28(U)	0.80(V)	0.84(V)	0.03(U)
	RSR	0.69(S)	0.73(U)	2.31(U)	0.45(V)	0.76(U)	1.06(U)	0.72(U)	0.64(S)	1.13(U)	0.44(V)	0.40(V)	0.98(U)
A5–A8	R^2	0.95	0.98	0.82	0.99	0.97	0.95	0.95	0.97	0.85	0.99	0.99	0.77
	NSE	0.95(V)	0.96(V)	0.31(U)	0.96(V)	0.86(V)	0.72(G)	0.92(V)	0.94(V)	0.72(G)	0.97(V)	0.95(V)	0.91(V)
	RSR	0.23(V)	0.19(V)	0.83(U)	0.21(V)	0.38(V)	0.53(G)	0.28(V)	0.24(V)	0.53(G)	0.17(V)	0.22(V)	0.30(V)
B5–B8	R^2	0.92	0.97	0.76	0.98	0.96	0.85	0.94	0.97	0.67	0.99	0.99	0.78
	NSE	0.81(V)	0.79(V)	−0.02(U)	0.91(V)	0.70(G)	0.31(U)	0.91(V)	0.95(V)	0.69(G)	0.99(V)	0.99(V)	0.95(V)
	RSR	0.43(V)	0.45(V)	1.01(U)	0.31(V)	0.55(G)	0.83(U)	0.29(V)	0.22(V)	0.56(G)	0.10(V)	0.11(V)	0.22(V)
C5–C8	R^2	0.96	0.99	0.87	0.99	0.97	0.93	0.94	0.98	0.63	0.99	0.99	0.67
	NSE	0.75(V)	0.73(G)	−0.07(U)	0.90(V)	0.68(G)	0.31(U)	0.83(V)	0.85(V)	0.51(S)	0.95(V)	0.93(V)	0.80(V)
	RSR	0.50(V)	0.52(G)	1.03(U)	0.32(V)	0.57(G)	0.83(U)	0.42(V)	0.39(V)	0.70(S)	0.23(V)	0.27(V)	0.44(V)
D5–D8	R^2	0.94	0.95	0.95	0.97	0.93	0.83	0.93	0.99	0.73	0.99	0.99	0.58
	NSE	−0.06(U)	0.03(U)	−5.12(U)	0.72(G)	0.32(U)	−0.68(U)	0.22(U)	0.32(U)	−0.39(U)	0.68(G)	0.73(G)	−0.86(U)
	RSR	1.03(U)	0.98(U)	2.47(U)	0.53(G)	0.83(U)	1.29(U)	0.88(U)	0.83(U)	1.18(U)	0.57(G)	0.52(G)	1.36(U)

Notes: LAI, Leaf Area Index; Stage-1: before maximum LAI; Stage-2: after maximum LAI; (V), very good; (G), good; (S), satisfactory; (U), unsatisfactory; A1–A8, B1–B8, C1–C8, D1–D8: plot names.

plots D5–D8 where the model performance is "unsatisfactory" and quite puzzling.

3.1.2. Soil water

The simulated soil water storages in the upper 0.6 m soil were compared to the observed ones (Figs. 3a and 3b). A8 represents irrigated plots and B4 non-irrigated plots. Linear regression analysis between the simulated and observed values was performed for all the plots except A5 in 2004 due to data absence. Values of R^2 were larger than 0.60 for 26 out of 31 plots in 2004, 29 out of 32 plots in 2005, respectively; and in most cases, the values are larger than 0.70. Error analysis indicated that the simulated soil water contents in the top 0.6 m layer were usually 8–12% lower than the observed values, with a standard deviation 6–4% in 2004 and 2005, respectively.

3.1.3. Evapotranspiration

No measured ET values from the 32 plots were available for evaluating the simulated ET. As an alternative, the measured ET data from the single lysimeter located on the experiment site was used to evaluate the simulated ET values of summer maize from multiple plots. The planting and harvest dates of summer maize were different between the experimental plots and the weighing lysimeter. For the 32 plots, summer maize was planted on June 10 and harvested on September 22; while for weighing lysimeter, summer maize was planted on June 21 and harvested on October 2. In order to eliminate the influences of different planting and harvesting dates on ET, the comparison was done for the different growth periods instead of day to day. The whole growth period of summer maize was divided into 11 growth stages, such as sowing, emergence, 3-leaf, 7-leaf, jointing, booting, heading, flowering, filling, milking and mature. All the indices all indicated very good agreement between the simulated and the measured ET of different growth periods (Table 3). The simulated seasonal ET was 408 mm for 2004 and 424 mm for 2005, and the measured was 402 mm and 416 mm for 2004 and 2005, respectively, representing a difference of only 1.5–1.9% between the simulated and measured ET values.

3.2. Regional water balance and temporal variations

3.2.1. Irrigation

Monthly and annual irrigation water amounts for each crop were compared among different irrigation scenarios over the study area. The annually averaged irrigation amounts for automatic irrigation (scenario 1) and different scheduled irrigation (scenarios 2–6) were compared in Fig. 4. The warm-up period ran from 1961 to 1968. Hence, comparisons were done for years from 1969 to 2005. For scenario 1, the mean annual irrigation water for all the crops over the study area was 130.9×10^8 m^3 (202 mm equivalent in water depth over the total study area) with standard deviation of 30.6×10^8 m^3 (47 mm). The significant variation of the annual irrigation (Coefficient of Variation $CV = 0.23$) is attributed to the variation of annual precipitation and atmospheric evaporative demand

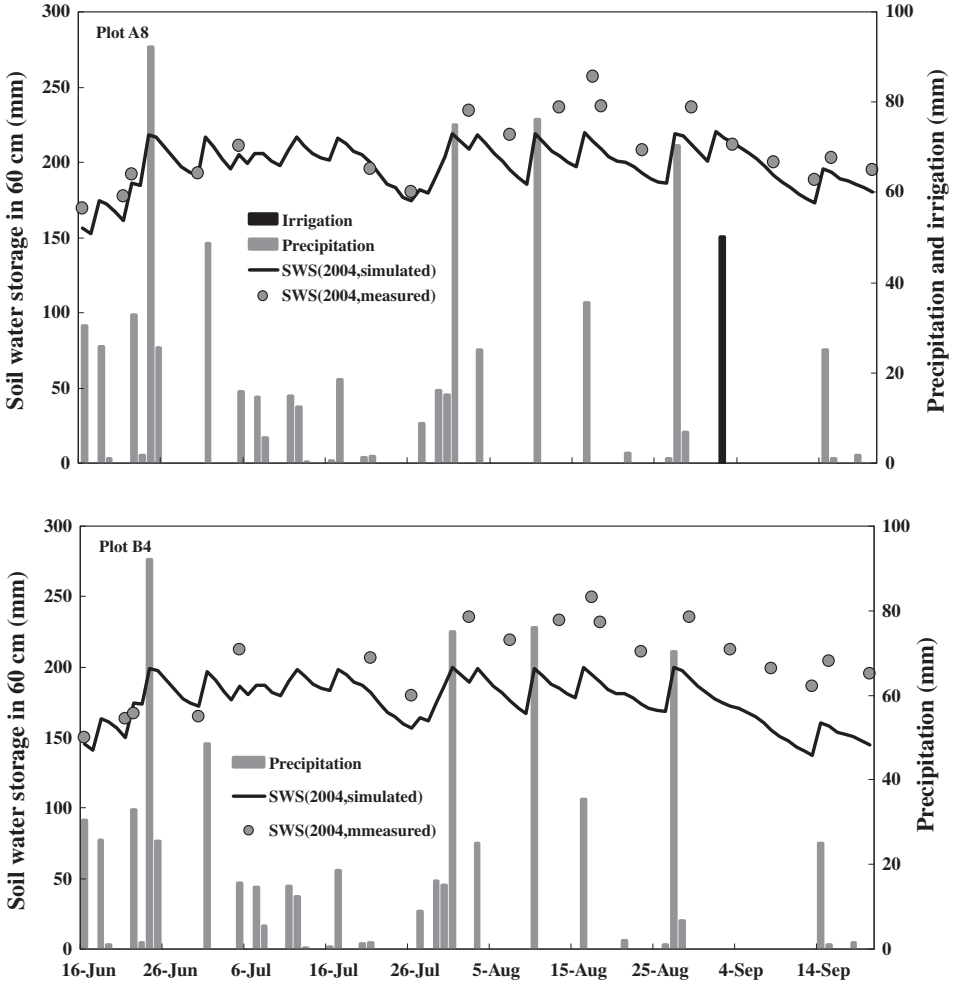

Fig. 3a. Comparison of simulated soil water storage (SWS) in the upper 60 cm layer to the measured one in 2004.

as the annual precipitation varied with a mean of 556 mm and coefficient of variation 0.26 over the period of 1969–2005. There is a negative relation between precipitation and total irrigation ($r = -0.68$, $P < 0.01$ under the automatic irrigation). In 1970, the annual precipitation was only 353 mm, and the irrigated water was as high as 188.6×10^8 m^3 (291 mm). However, in 1990, the applied irrigation only amounted to 52.0×10^8 m^3 (80 mm) when annual precipitation reached 735 mm. Irrigation could also be very high when the precipitation was abundant, but much of it occurred just after irrigation. For example, irrigation water was 144.0×10^8 m^3 with 630 mm precipitation in 1982, and 160.0×10^8 m^3 with 774 mm precipitation in 2000. In practice, farmers will not irrigate crops right after the soil water is supplemented by a rainfall event. Irrigation is also affected by the seasonal distribution of precipitation. Compared to the irrigation amount in 1990, the amount of irrigation applied from March to June in 2000 had increased by 148% and from July to September by 684%. During the same seasons, the amount of precipitation was: 217 mm in 1990 and 56 mm in 2000 for the period of March to June; 420 mm in 1990 and 593 mm in 2000 for the period of July to September; but 139 mm in 1990 and only 10 mm in 2000 for August. The low precipitation in August 2000 led to the large increase of irrigation for the period of July to September in the same year. For scheduled irrigation scenarios, annual irrigation amount almost remained unchanged for the period of 1969–2005. Annual average irrigation under scenarios 2–6 amounted to 86.6×10^8 m^3 (134 mm), 75.6×10^8 m^3 (117 mm), 69.8×10^8 m^3 (108 mm), 58.7×10^8 m^3 (91 mm), and 65.2×10^8 m^3 (101 mm), respectively, representing a decrease of 33.9%, 42.3%, 46.7%, 55.2%, and 50.2%, respectively, compared to the automatic irrigation scenario (scenario 1). It should be noted that the scheduled irrigation was always applied on the predefined date and the predefined irrigation schedules remained unchanged during the simulations by the SWAT model. The scheduled irrigation module needs to be improved to handle various irrigation dates flexibly for better representation of irrigation practices.

Fig. 5 shows the monthly precipitation and irrigation amounts under different scenarios for the three main crops: wheat, maize, and cotton. The simulated irrigation amount was largest in March for wheat, July for summer maize, and April for cotton. For these three crops, the SWAT model automatically starts irrigation when the soil water content touches the predefined threshold value of 80% of the field capacity without considering the proper irrigation

Table 3
Statistical summary of the simulated against observed evapotranspiration for summer maize at different growth stages in 2004 and 2005.

	NSE	RSR	R^2
2004	0.94(V)	0.23(V)	0.94
2005	0.90(V)	0.30(V)	0.92

Note: NSE, Nash–Sutcliffe efficiency; RSR, the ratio of the root mean square error to the standard deviation of measured data; R^2, and coefficient of determination; (V), very good.

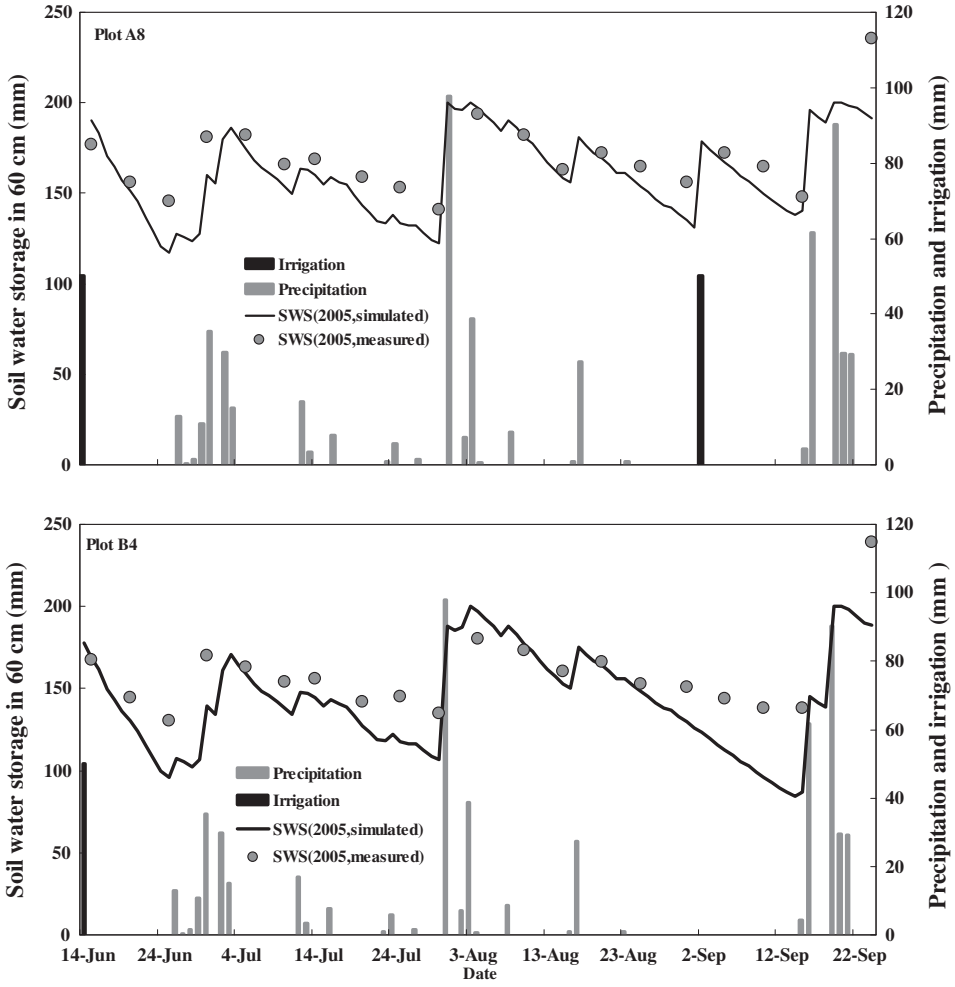

Fig. 3b. Comparison of simulated soil water storage (SWS) in the upper 60 cm layer to the measured one in 2005.

time and amount agronomically. This limit of the SWAT model may also be attributed to why irrigation applications were found during both the weak water demand seasons of crops (e.g., June and December) and during the abundant precipitation season (e.g., July and August). Winter wheat is usually harvested in the early or middle June. No irrigation is needed for the winter wheat in maturity. Summer maize is typically sown right after the harvest of the winter wheat. It is only in very dry seasons that irrigation may be applied for the summer maize at seeding and emergence stages in June. No irrigation is needed for summer maize and cotton in July and August with abundant precipitation. Irrigation amount of the scenario 1 seemed quite excessive than what was needed by both farming practices and our field experiments. It sets up an upper limit of irrigation water amount under the local conditions. For the scheduled irrigation scenarios 2–6, annual irrigation water amount remained the same as that designed in the irrigation schedules except in the years 1993 and 1998 (Fig. 4). In the SWAT model, the amount of each irrigation is predefined in its management file. When irrigation option is executed, water infiltrates the unsaturated soil top down. If excessive water (i.e., predefined irrigation amount exceeds the amount of water needed to fill the soil water deficit) exists, the SWAT model assumes that the excessive part goes back to the original water sources. The part that is added to the soil profile is considered as the 'irrigation' amount. The simulation results indicate that the 'excessive amount' occurred in both 1993 and 1998. Generally, the results showed that the defined irrigation schedules reflected the normal practices of the study area.

3.2.2. Evapotranspiration

Statistical results of ET for winter wheat, summer maize, and cotton under different irrigation scenarios are given in Table 4. The results indicate that irrigation had significant impacts on the crop ET. For winter wheat, the mean seasonal ET of the scenarios 1–3 were larger than the reported value of 452 mm (Wu, 2003); however, ET of the scenarios 2 and 3 with winter irrigation was approximately 59 mm more than the scenarios 4–6 without winter irrigation. ET of the scenarios 2 and 3 were 14 mm larger than that under full irrigation (scenario 1) with winter irrigation (Fig. 6). ET from December 10 to March 31 under scenario 1 (automatic irrigation) was 37 mm lower than that under scenario 2 (scheduled irrigation) with winter irrigation on December 10 and once irrigation on March 15. The seasonal ET of every irrigated scenario was two to three times of the precipitation amount during the same period. Even if no irrigation was applied (scenario 7), the seasonal ET was approximately 110 mm more than the 155 mm precipitation during the same period, which implied the winter wheat made use of the preseason soil water storage.

For the summer maize, however, the seasonal ET was only 310 mm when no irrigation was applied, which was far less than the 350 mm precipitation during the same period. This strongly indicates that summer maize might experience soil water stress and supplemental irrigation is necessary.

Sequential planting of the winter wheat and summer maize is the most common system in the study area. The annual ET of winter wheat and summer maize for different irrigation scenarios ranged from 578 mm to 897 mm. The annual precipitation can meet 96% of the crop ET because crop evapotranspiration was quite low under water stress condition when no irrigation was applied; and 62% of the crop ET when crop evapotranspirated more under non-water stress condition. Practically, the scheduled irrigation scenarios were commonly adopted around the study area depending upon the water supply situation. The automatic irrigation and no irrigation scenarios were purely set as reference lines for analyzing crop water use in this study. Therefore, the annual precipitation could guarantee 62–96% of the double-cropping water requirements of wheat and maize rotation, dependent upon different irrigation schedules. However, during the winter wheat season, the precipitation could only meet with 32–36% of the crop water requirement and the percentage varied with the different irrigation schedules.

The seasonal ET of cotton varied from 429 mm under no irrigation option to 624 mm under automatic irrigation option (Table 4). Cotton evapotranspirated 488 mm when sowing irrigation was applied and 551 mm when it was irrigated at bud stage too. The averaged seasonal precipitation was 477 mm. It appears that cotton crop does not need any supplemental irrigation at all. However, uneven distribution of precipitation during the growth season and variation among years make irrigation for cotton still necessary as the farmers' experience indicate. For the scheduled irriga-

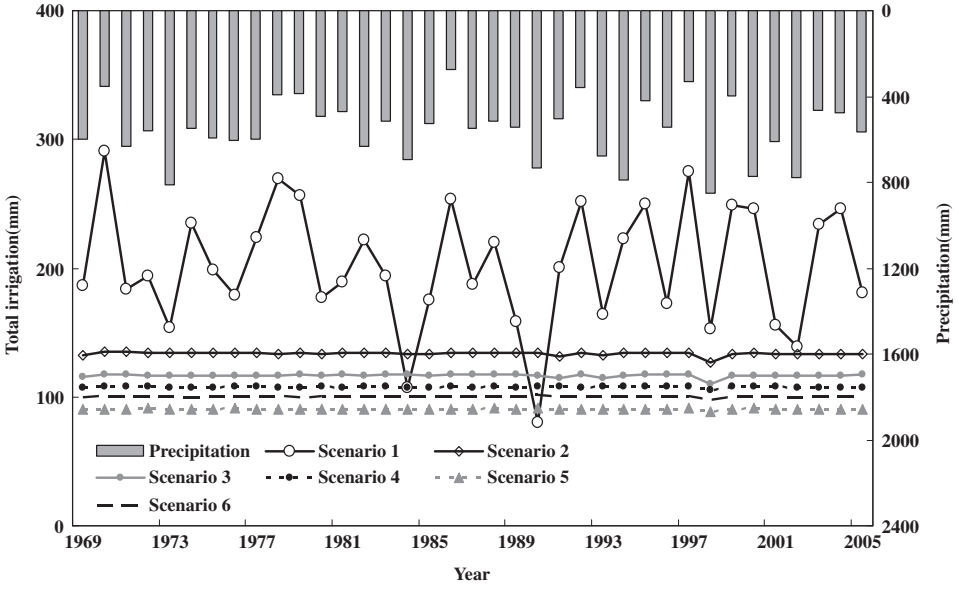

Fig. 4. The annual variation of precipitation and the simulated annual irrigation water amount under different scheduled irrigation scenarios (scenarios 1–6) from 1969 to 2005.

tion scenarios, precipitation can meet 87–98% of crop water requirement on the seasonal basis, and 101–114% on the annual basis. This might be an important reason that cotton is more popularly planted in areas where diversion water from river is not easily accessible and groundwater is usually not suitable for irrigation due to salts, e.g. in counties of Ningjin, Xiajin, Wucheng, and etc.

3.2.3. Runoff

Annual surface runoff and its variation under different scenarios are shown in Fig. 7. The scenarios 1 and 7 defined the upper and lower limits of the annual runoff volumes of the scenarios 1–7, respectively. Under conditions of the full irrigation scenario 1, the annual runoff reached up to 105 mm (68.0×10^8 m^3), which accounts for 19% of the mean annual precipitation, while 11% under the no irrigation scenario 7. For the scheduled irrigation scenarios 2–6, runoff volume accounted for 13% of the precipitation on average and was, closer to that of the no irrigation scenario. In the SWAT model, irrigation water is not allowed to generate runoff, the excessive water beyond irrigation requirement was assumed to go back to the source. However, irrigation may influence

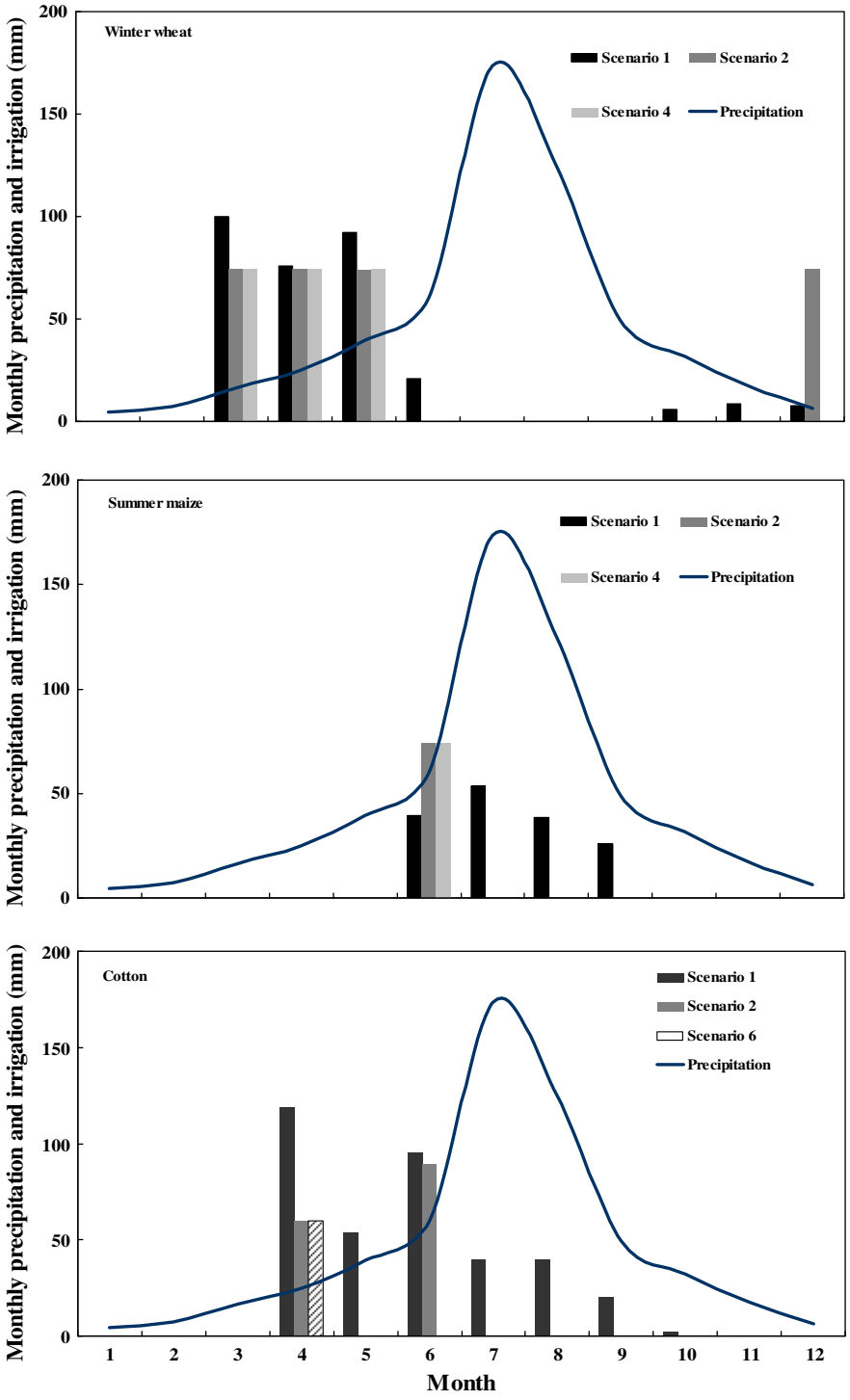

Fig. 5. The month precipitation and the simulated month irrigation water amount for winter wheat, summer maize and cotton under different irrigation scenarios (scenarios 1–6) from 1969 to 2005.

runoff generation through increasing the soil water content. This might be the main reason for the largest runoff volume under the scenario 1 which keeps the soil water storage always above 80% of the field capacity.

Annual runoff volume is closely related to annual precipitation amount. Linear regression analysis between the annual runoff and precipitation indicated that the coefficients of determination were 0.78 for scenarios 1–6 and 0.77 for scenario 7, respectively (significant at $P < 0.01$). About 70% of the annual runoff occurred during months of July and August (Fig. 8) due to the concentrated precipitation, which accounted for 54% of its annual value. Irrigation (Fig. 5) enriched the soil water content and consequently, caused the differences of runoff volume among irrigation scenarios (Fig. 8). The more the irrigation was, the more the runoff generated. In other months, the difference was minor because of much less rainfall and hence, much less runoff.

Runoff could be intercepted by the canals or lost through transmission. Taken the outflow at outlets of the Tuhai river and the Majia river as an example, 52% for scenario 1, and 66% for scenarios 2–6 of the total runoff were intercepted by canals or lost through transmission, respectively, by comparing the flows at the outlets and the generated runoff volume (Table 5).

Table 4
Statistical summary of the simulated actual evapotranspiration of the major crops under different irrigation scenarios (mm).

	Scenarios	Mean (mm)	Maximum (mm)	Minimum (mm)	St. dev. (mm)	CV
Winter wheat	1	472	565	380	45	0.10
	2	485	575	413	45	0.09
	3	484	574	413	46	0.09
	4	426	528	344	48	0.11
	5	425	528	342	48	0.11
	6	426	528	344	48	0.11
	7	265	371	151	57	0.21
Summer maize	1	416	480	318	38	0.09
	2	409	475	325	31	0.08
	3	364	475	297	37	0.10
	4	406	476	325	31	0.08
	5	359	475	291	38	0.11
	6	406	476	325	31	0.08
	7	310	466	219	51	0.16
Winter wheat + summer maize	1	890	1008	698	74	0.08
	2	897	1018	774	59	0.07
	3	851	971	759	62	0.07
	4	835	968	735	60	0.07
	5	786	919	671	66	0.08
	6	835	968	735	60	0.07
	7	578	713	414	85	0.15
Cotton	1	624	714	538	41	0.07
	2	551	639	457	48	0.09
	3	551	639	457	48	0.09
	4	551	639	457	48	0.09
	5	551	639	457	48	0.09
	6	488	610	368	59	0.12
	7	429	566	309	61	0.14

Note: St. dev., standard deviation; CV, coefficient of variation.

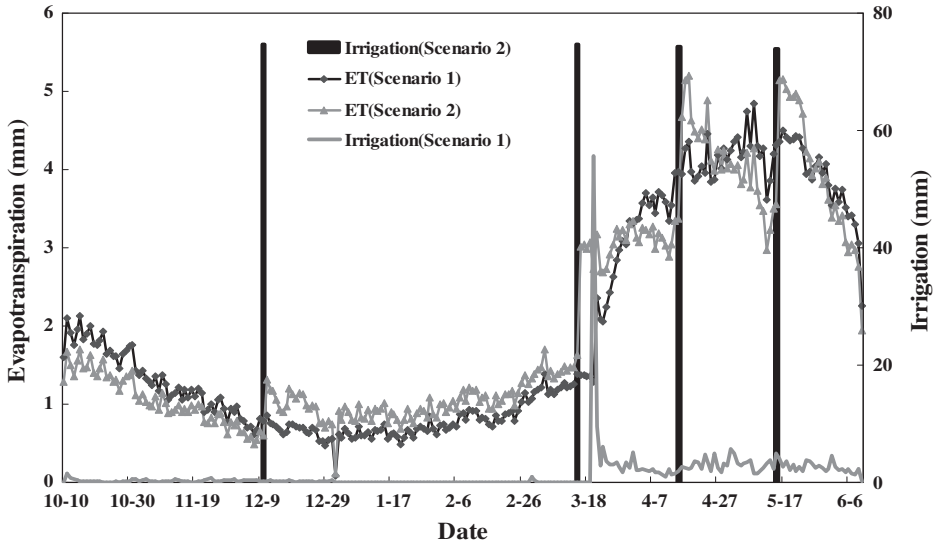

Fig. 6. Evapotranspiration and irrigation of winter wheat under scenarios 1 and 2 during winter wheat growth season.

3.3. Canal water balance and temporal variations

The simulated annually averaged water balance components of canals for the period of 1969–2005 were given in Table 6. In Table 6, the inflow water ratio (*FWR*), canal irrigation water ratio (*IWR*), seepage water ratio (*SWR*), and outflow water ratio (*OWR*) are defined as following, respectively.

$$FWR = \frac{Q_{flwi}}{Q_{div} + \beta \times Q_{flwi}} \tag{15}$$

$$IWR = \frac{Q_{irr}}{Q_{div} + \beta \times Q_{flwi}} \tag{16}$$

$$SWR = \frac{SEP}{Q_{div} + \beta \times Q_{flwi}} \tag{17}$$

$$OWR = \frac{Q_{flwo}}{Q_{div} + \beta \times Q_{flwi}} \tag{18}$$

The variables in Eqs. (15)–(18) are the same as in Eq. (1). The constant β was set as zero for Henan province where no CIDS canals were adopted and as one for Shandong province where CIDS canals were adopted.

Diversion water from the Yellow River for Shandong province was 54.0×10^8 m^3 for the automatic irrigation scenario; and 30.6×10^8 m^3 on average for the scheduled irrigation scenarios.

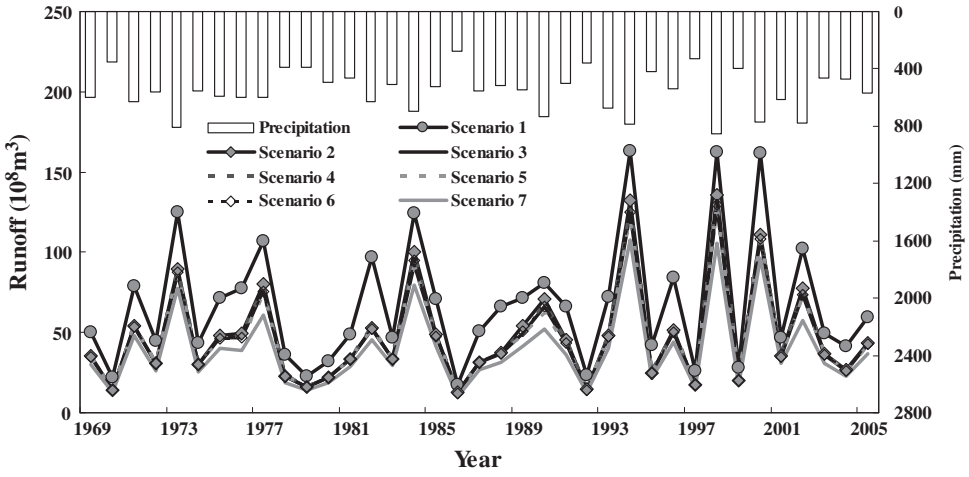

Fig. 7. Comparison of annually averaged surface runoff under different irrigation scenarios.

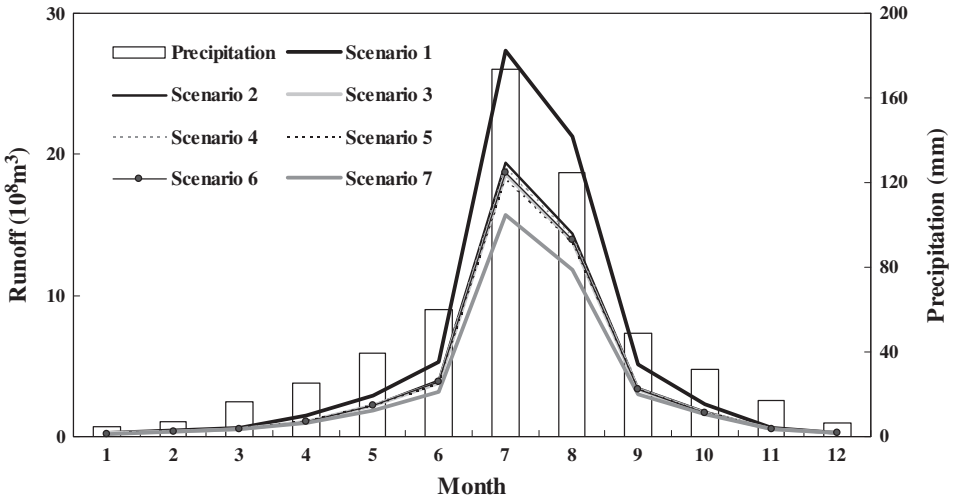

Fig. 8. Comparison of the monthly averaged surface runoff under different irrigation scenarios.

Table 5
Comparison between the simulated runoff and the outflow at outlets of two example streams under different irrigation scenarios. The quantities are given in water depth with respect to the area which river flows through, mm.

Outlets	Scenario 1		Scenario 2		Scenario 3		Scenario 4		Scenario 5		Scenario 6	
	RF	SF	RF	SF	RF	SF	RF	SF	RF	SF	RF	SF
Tuhai River	88.5	42.6	64.7	20.3	62.7	18.6	63.7	19.5	62.2	20.3	63.3	18.9
Majia River	99.9	48.1	66.8	25.1	64.3	23.5	65.4	24.4	63.3	25.1	64.7	24.0

Note: RF, runoff; SF, stream flow.

Table 6
Statistical analysis of water balance components (WBC) of canals (10^8 m^3).

	WBC	Scenarios											
		1	2	3	4	5	6	8	9	10	11	12	13
Whole region	Q_{div}	59.3	55.4	52.4	52.3	49.2	51.5	0.0	0.0	0.0	0.0	0.0	0.0
	$\beta \times Q_{flwi}$	56.6	41.6	39.7	40.5	38.7	39.7	57.5	41.9	39.9	40.7	38.9	39.9
	Q_{irr}	64.4	42.8	37.6	37.2	31.9	35.7	15.8	11.8	11.2	8.8	8.3	8.5
	E	2.2	3.0	3.1	3.1	3.2	3.2	1.6	1.4	1.4	1.5	1.5	1.5
	SEP	21.2	26.7	27.2	28.3	28.9	28.4	12.8	10.3	10.3	12.4	12.4	12.4
	Q_{flwo}	28.0	24.5	24.2	24.1	23.9	23.9	27.3	18.5	17.0	17.9	16.4	17.4
	ΔV	0.00	0.00	0.01	0.00	0.00	0.00	0.00	0.00	0.00	0.10	0.20	0.10
	FWR	0.49	0.43	0.43	0.44	0.44	0.44	1.00	1.00	1.00	1.00	1.00	1.00
	IWR	0.56	0.44	0.41	0.40	0.36	0.39	0.27	0.28	0.28	0.22	0.21	0.21
	SWR	0.18	0.27	0.29	0.31	0.33	0.31	0.22	0.24	0.26	0.30	0.32	0.31
	OWR	0.24	0.25	0.26	0.26	0.27	0.26	0.48	0.44	0.43	0.44	0.42	0.44
Part in Shandong province	Q_{div}	41.1	37.8	35.4	35.1	32.6	34.3	0.0	0.0	0.0	0.0	0.0	0.0
	$\beta \times Q_{flwi}$	56.6	41.6	39.7	40.5	38.7	39.7	57.5	41.9	39.9	40.7	38.9	39.9
	Q_{irr}	55.0	35.5	31.2	30.7	26.4	29.3	15.8	11.8	11.2	8.8	8.3	8.5
	E	1.8	2.5	2.5	2.6	2.6	2.6	1.6	1.4	1.4	1.5	1.5	1.5
	SEP	13.8	16.9	17.1	18.2	18.4	18.2	12.8	10.3	10.3	12.4	12.4	12.4
	Q_{flwo}	28.0	24.5	24.2	24.1	23.9	23.9	27.3	18.5	17.0	17.9	16.4	17.4
	ΔV	0.01	0.00	0.00	0.01	0.00	0.00	0.00	0.00	0.00	0.10	0.20	0.10
	FWR	0.58	0.52	0.53	0.54	0.54	0.54	1.00	1.00	1.00	1.00	1.00	1.00
	IWR	0.56	0.45	0.42	0.41	0.37	0.40	0.27	0.28	0.28	0.22	0.21	0.21
	SWR	0.14	0.21	0.23	0.24	0.26	0.25	0.22	0.24	0.26	0.30	0.32	0.31
	OWR	0.29	0.31	0.32	0.32	0.34	0.32	0.48	0.44	0.43	0.44	0.42	0.44
Part in Henan province	Q_{div}	18.2	17.6	17.0	17.2	16.7	17.1						
	$\beta \times Q_{flwi}$	0.0	0.0	0.0	0.0	0.0	0.0						
	Q_{irr}	9.4	7.3	6.4	6.5	5.5	6.4						
	E	0.4	0.6	0.6	0.6	0.6	0.6						
	SEP	7.4	9.7	10.1	10.1	10.5	10.2						
	Q_{flwo}	0.0	0.0	0.0	0.0	0.0	0.0						
	ΔV	0.00	0.00	0.00	0.00	0.00	0.00						
	IWR	0.52	0.41	0.37	0.38	0.33	0.37						
	SWR	0.41	0.55	0.59	0.59	0.63	0.59						
	OWR	0.00	0.00	0.00	0.00	0.00	0.00						

Note: WBC, water balance components; Q_{div}, actual annual diversion water; β, constant; Q_{flwi}, inflow water; Q_{irr}, irrigation water from the canals; E, evaporation, SEP, seepage from the canals; Q_{flwo}, outflow water; V, change of the canal water storage; FWR, inflow water ratio; IWR, irrigation water ratio; SWR, seepage water ratio; OWR, outflow water ratio.

The inflow water Q_{flwi} including the intercepted surface runoff and collected drainage from cropland varied with irrigation schedules and irrigation water sources. The inflow of automatic irrigation was much larger than that of scheduled irrigations because surface runoff and field drainage of the former were much larger than that of the later ones. The inflow did not show significant difference among the scheduled irrigation scenarios. For the scenarios that used surface and groundwater as irrigation sources, the inflow

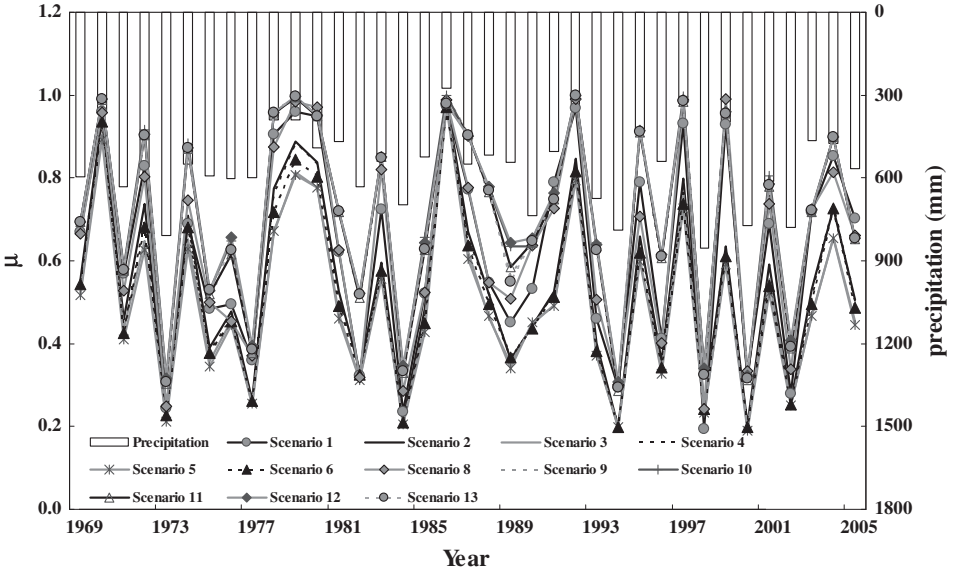

Fig. 9. Comparison of the annual average interception ratio of runoff and drainage of the combined irrigation, drainage, and storage canals under different irrigation scenarios.

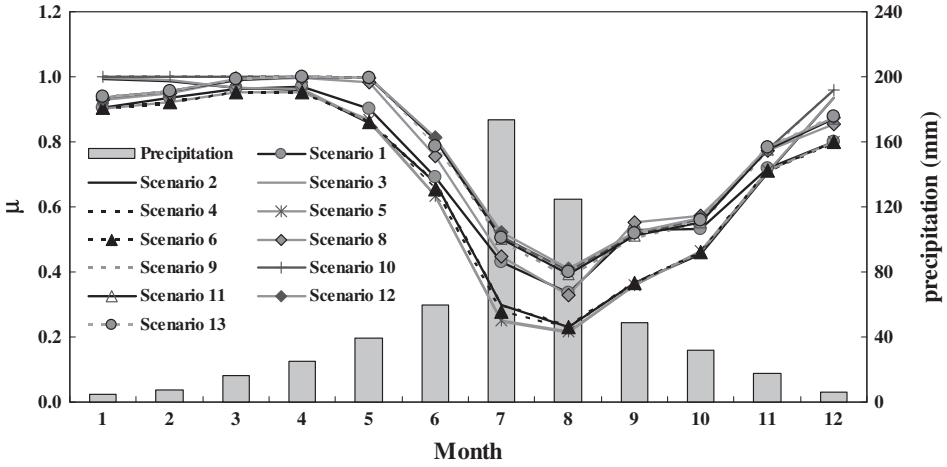

Fig. 10. Comparison of the monthly average interception ratio of runoff and drainage from cropland of the combined irrigation, drainage, and storage canals under different irrigation scenarios: μ is defined as ratio of the intercepted surface runoff and field drainage to the total surface runoff and field drainage.

water ratio got to approximately 0.54 which implied the same importance of the CIDS canal in both storing water for irrigation and delivering the diversion water in Shandong province where the CIDS canal is commonly adopted.

Annually averaged *IWR* values over the whole region and in Shandong and Henan provinces did not show significant differences, although the value was slightly higher in Shandong than in Henan. The *IWR* values were influenced by irrigation management. Under the scenarios 1–6, the *IWR* values decreased significantly from the scenario 1 to scheduled irrigation scenarios (scenarios 2–6). The low *IWR* in the irrigation districts was mostly attributed to transmission loss of canal, mainly the seepage. With decreasing *IWR,* values of *SWR* increased correspondingly (Table 6). Seepage recharges the shallow aquifer, and in turn is to be reused later (Bouarfa et al., 2006). The water flowing out of the canal system accounted for approximately 32% of the input water including both the diversion from the Yellow River and the intercepted water by the CIDS canals.

The ratios of seepage varied irrigation scenarios and were different between regions with CIDS canals or without CIDS canals. In the part of Henan province without the CIDS canals, the averaged ratio of seepage for the simulated scenarios was 0.59. However, the value was 0.24 in the part of Shandong province where the CIDS canals were commonly adopted due to inclusion of the intercepted surface runoff and drainage from the cropland in the seepage ratio, which implied that the storage function of the CIDS canals played a role of temporal regulation of the surface water for irrigation (Table 6). Anyway, the seepage that goes into shallow aquifer is to be reused later for irrigation (Bouarfa et al., 2006), and therefore, enhances the water resources efficiency consequently.

3.4. Drainage collection and runoff interception by the CIDS canals

An index ω is used to express the ratio of surface runoff and drainage collected by the CIDS canals to the irrigation water amount drawn from the CIDS canals.

$$\omega = \frac{\beta \times Q_{retent}}{Q_{irr}} \tag{19}$$

where Q_{retent} is the surface runoff and field drainage intercepted by canals (m^3), other variables were defined in Eq. (1). ω was approximately 0.53 for the full irrigation (scenario 1), and 0.48, 0.50, 0.53, 0.56 and 0.54 for scheduled irrigation conditions (scenarios 2–6), respectively, indicating that the CIDS canals played an important role in supplying water for irrigation. Scenarios 8–13 assumed that irrigation used the canal water and groundwater but no diversion water from the Yellow River was available. Volumes of surface runoff and field drainage intercepted by the CIDS reached approximately 24.0×10^8 m^3 under scenarios 8–13, but only a small part was used for irrigation, e.g., 15.8×10^8 m^3 for scenario 8, 11.5×10^8 m^3 for scenarios 9 and 10, and 8.4×10^8 m^3 in scenarios 11–13. Mostly, the water recharged the shallow aquifer and flew out of the study area (Table 6).

An index μ, defined as the ratio of runoff and field drainage received by canals to the total runoff and field drainage produced in the study area, is used to evaluate the amount of runoff and field drainage intercepted by the canals.

$$\mu = \frac{Q_{retent}}{R + Drainage} \tag{20}$$

where R is the runoff volume generated in the study area (m^3), *Drainage* is the field drainage generated in the study area (m^3).

Figs. 9 and 10 showed the annual variation and monthly variation of the index μ, respectively. Generally, μ was larger in the case of no diverting water from the Yellow River (approximately 0.69 under scenarios 8–13) than in the case of diverting water from the Yellow River (0.53 under scenarios 1–6). Annually and monthly averaged values of μ were linearly correlated to precipitation ($r = -0.86$ and -0.76, $P < 0.01$). In some years with less precipitation, such as 1970, 1979, 1986, 1992, μ got as high as 0.95 implying almost total interception of the surface runoff and drainage from the cropland by the CIDS canals. While in some years with abundant precipitation, for example, averaged μ was just around 0.26 in 1984, 1994, 1998, and 2000, which implied either the volume of the surface runoff and drainage from the cropland surpassed the storage capacities of the CIDS canals or partial occupation of the storage capacity of the CIDS by the diversion water from the Yellow River. Proper maintenance of the storage capacity of the CIDS is likely to increase reusing the surface runoff and field drainage for irrigation supply (Bouarfa et al., 2006).

4. Conclusions

A new module for simulating CIDS (combined irrigation, drainage, and storage) canals was developed for the SWAT2000 model in this paper. It considers both surface runoff and drainage from croplands in computing the water balance of the CIDS canals. The improved SWAT model was calibrated and evaluated with the field experiment data and employed to simulate the multiple roles of

the CIDS canals under different irrigation scenarios in the irrigation districts along the lower Yellow River.

The simulated results show that the averaged annual irrigation for all crops over the study area was the highest under the full irrigation (automatic irrigation option) scenario and much lower under the scheduled irrigation scenarios. Generally, irrigation water amount was negatively correlated to the precipitation amount, and could also be very high when the precipitation was abundant but occurred untimely.

The annual ET of the double-cropping winter wheat and summer maize was the highest (897 mm) under the full irrigation scenario and the lowest (578 mm) when no irrigation was applied, and varied between these two values when other irrigation schedules were adopted. Precipitation could meet the water requirement of the double-cropping system by 62–96% on an annual basis; that of the winter wheat by 32–36%, summer maize by 92–123%, and cotton by 87–98% on a seasonal basis. Hence, timely irrigation for winter wheat is critical to ensure high wheat yield.

Runoff generation was closely related to precipitation and influenced by irrigation. The highest (105 mm, or 6.80×10^9 m^3) and lowest (61 mm, or 3.98×10^9 m^3) annual runoff accounted for 19% and 11% of the annual precipitation under the full irrigation and no irrigation scenarios, respectively. For the scheduled irrigation scenarios, runoff volume accounted for 13% of the precipitation on average. Nearly 70% of the annual runoff occurred during months of July and August due to the concentrated precipitation in these 2 months.

The CIDS canals played an important role in intercepting the surface runoff and drainage from cropland (inflow of the CIDS canal) and recharging the shallow aquifer for later use. The ratio of inflow to the total amount of diversion plus inflow was as high as approximately 0.54, which implied the same importance of the CIDS canal in both storing water for irrigation and delivering the diversion water in Shandong province where the CIDS canal is commonly adopted. Roughly 14–26% of the total flow (diversion water and the intercepted surface runoff and drainage from cropland) in the CIDS canal system recharged shallow aquifer through canal seepage. The water flowing out of the canal system accounted for approximately 32% of the water (diversion plus inflow) in the CIDS canals.

The ratio of intercepted runoff and collected drainage to the total runoff and drainage generated in the study area was negatively correlated to the precipitation. In years with abundant precipitation, the volume of the surface runoff and drainage from the cropland may surpass the storage capacities of the CIDS canals, while in years with less precipitation, partial storage capacity of the CIDS canal may be occupied by the diversion water from the Yellow River. Proper maintenance of the storage capacity of the CIDS has the potential in improving the efficiency of reusing the surface runoff and field drainage for irrigation practice to mitigate the increasing water shortage along the lower Yellow River.

Acknowledgements

This research was partially financed by the Natural Sciences Foundation of China (No. 90502005), the National 863 High-tech Program of China (No. 2007AA10Z223), and the National Basic Research Program of China (No. 2005CB121103).

References

Allen, R.G., 1986. A Penman for all seasons. Journal of Irrigation and Drainage Engineering ASCE 112 (4), 348–368.

Allen, R.G., Jensen, M.E., Wright, J.L., Burman, R.D., 1989. Operational estimates of evapotranspiration. Agronomy Journal 81, 650–662.

Arnold, J.G., Allen, P.M., 1996. Estimating hydrologic budgets for three Illinois watershed. Journal of Hydrology 176, 57–77.

Bouarfa, S., Vincent, B., Wu, J., Yang, J., Zimmer, D., 2006. Role of groundwater in irrigation water management in the downstream part of the Yellow River. Irrigation and Drainage Systems 20, 247–258.

Chu, T.W., Shirmohammadi, A., Montas, H., Sadeghi, A., 2004. Evaluation of the SWAT model's sediment and nutrient components in the piedmont physiographic region of Maryland. Transactions of the ASAE 47 (5), 1523–1538.

Department of Water Resources of Henan Province, 1985–1992. Henan Water Resources Statistical Yearbook.

Department of Water resources of Shandong Province, 1985–1992. Shandong Water Resources Statistical Yearbook.

Fang, Q.X., Chen, Y.H., Li, Q.Q., Yu, S.H., Luo, Y., Yu, Q., Ouyang, Zh., 2004. Effect of irrigation on water use efficiency of winter wheat. Transactions of the CSAE 20 (4), 34–39 (in Chinese).

Fang, Q., Ma, L., Yu, Q., Ahuja, L.R., Malone, R.W., Hoogenboom, G., 2009. Irrigation strategies to improve the water use efficiency of wheat–maize double cropping systems in North China Plain. Agricultural Water Management 12, 14–25. doi:10.1016/j.agwat.2009.02.012.

Fang, Q.X., Ma, L., Green, T.R., Yu, Q., Wang, T.D., Ahuja, L.R., 2010. Water resources and water use efficiency in the North China Plain: current status and agronomic management options. Agricultural Water Management 12, 23–32. doi:10.1016/j.agwat.2010.01.008.

Gassman, P.W., Reyes, M.R., Green, C.H., Arnold, J.G., 2007. The soil and water assessment tool: historical development, applications, and future research directions. Transactions of ASABE 50 (4), 1211–1250.

Gosain, A.K., Rao, S., Srinivasan, R., Reddy, N.G., 2005. Return-flow assessment for irrigation command in the Palleru river basin using SWAT model. Hydrological Processes 19, 673–682.

Henan Rural Social and Economic Survey Team, 2001. Henan Rural Statistical Yearbook (2001). China Statistics Press, Beijing, China.

Hou, Chuanhe, Xiao, Sujun, Hou, Yuling, 2000. Analysis of water resources and its utilization characteristics in the irrigation areas along the lower reaches of the Yellow river. Irrigation and Drainage 19 (3), 62–65 (in Chinese).

Leavesley, G.H., Lichty, R.W., Troutman, B.M., Saindon, L.G., 1983. Precipitation-runoff Modeling System: User's Manual. US Geological Survey. Water-Resources Investigations Report 83-4238, 207pp.

Li, Q.Q., Chen, Y.H., Liu, M.Y., Zhou, X.B., Yu, S.L., Dong, B.D., 2008. Effects of irrigation and planting patterns on radiation use efficiency and yield of winter wheat in North China. Agricultural Water Management 95, 469–476.

Liu, Y., Cai, J.B., Cai, L.G., Pereira, L.S., 2005. Analysis of irrigation scheduling and water balance for an irrigation district at lower reaches of the Yellow River. Journal of Hydraulic Engineering 36 (6), 701–708 (in Chinese).

Liu, Y.J., Luo, Y., 2010. A consolidated evaluation of the FAO-56 dual crop coefficient approach using the lysimeter data in the North China Plain. Agricultural Water Management 97, 31–40.

Luo, Y., He, Chansheng, Sophocleous, M., Yin, Zhi Fang, Ren, Hong Rui, Ouyang, Zhu, 2008. Assessment of crop growth and soil water modules in SWAT2000 using extensive field experiment data in an irrigation district of the Yellow River Basin. Journal of Hydrology 352, 139–156.

Minhas, P.S., Tyagi, N.K., Gupta, S.K., Dong, K.L., Cai, L.G., Pereira, L.S., 2006. Assessing drainage water reuse options in Bojili irrigation district, Shandong. Irrigation and Drainage 55, 463–477.

Ministry of Water Resources of China, 1994. The Handbook of Irrigation Management. China Water Power Press, Beijing, China.

Monteith, J.L., 1965. Evaporation and the environment. In: XIXth Symposium, Soc. Exp. Biol., Swansea. Cambridge University Press.

Moriasi, D.N., Arnold, J.G., Van Liew, M.W., Bingner, R.L., Harmel, R.D., Veith, T.L., 2007. Model evaluation guidelines for systematic quantification of accuracy in watershed simulations. Transactions of the American Society of Agricultural and Biological Engineers 50 (3), 885–900.

Neitsch, S.L., Arnold, J.G., Kiniry, J.R., Williams, J.R, King, K.W., 2002. Soil and Water Assessment Tool Theoretical Documentation, Version 2000. Grassland, Soil and Water Research Laboratory, Agricultural Research Service, 808 East Blackland Road, Temple, TX. <http://www.brc.tamus.edu/swat/>.

Pereira, L.S., Cai, L.G., Musy, A., Minhas, P.S. (Eds.), 2003. Water Savings in the Yellow River Basin. Issues and Decision Support Tools in Irrigation. China Agriculture Press, Beijing. 291p.

Perkins, S.P., Sophocleous, M., 2000. Combining SWAT and MODFLOW into an Integrated Watershed Model. Open-File Report No. 2000–67, Kansas Geological Survey. The University of Kansas, Lawrence, KS 66047.

Querner, E.P., Morábito, J.A., Manzanera, M., et al., 1997. The use of hydrological models in the irrigated areas of Mendoza, Argentina. Agricultural Water Management 35, 11–28.

Ren, W., Yao, K.M., Yu, Q., Ouyang, Zh., Wang, L., 2003. Effect of water control in combination of depth and amount on dry matter partition and water use efficiency of winter wheat. Chinese Journal of Eco-agriculture 11 (4), 92–94 (in Chinese).

Ritschard, R.L., Cruise, J.F., Hatch, L.U., 1999. Spatial and temporal analysis of agricultural water requirements in the Gulf Coast of the United States. Journal of the American Water Resources Association 35 (6), 1585–1596.

Rosenthal, W.D., Hoffman, D.W., 1999. Hydrologic modeling/GIS as an aid in locating monitoring sites. Transactions of the ASAE 42 (6), 1591–1598.

Santhi, C., Muttiah, R.S., Arnold, J.G., Srinivasan, R., 2005. A gis-based regional planning tool for irrigation demand assessment and saving using SWAT. Transactions of the ASAE 48 (1), 137–147.

Shandong Bureau of Statistics, 2001. Shandong Rural Statistical Yearbook (2001). China Statistics Press, Beijing, China.
Shao, L.W., Zhang, X.Y., Chen, S.Y., Sun, H.Y., Pei, D., 2009. Yield and water use efficiency affected by rainfall, irrigation and maize varieties. Journal of Irrigation and Drainage 28 (1), 48–51 (in Chinese).
Sophocleous, M., Perkins, S.P., 1999. Development of a comprehensive watershed model applied to study stream yield under drought conditions. Ground Water 37 (3), 418–426.
Sophocleous, M., Perkins, S.P., 2000. Methodology and application of combined watershed and ground-water models in Kansas. Journal of Hydrology 236, 185–201.
Spruill, C.A., Workman, S.R., Taraba, 2000. Simulation of daily and monthly stream discharge from small watersheds using the SWAT model. Transactions of the ASAE 43 (6), 1431–1439.
Streeter, V.L., Wylie, E.B., 1979. Fluid Mechanic. McGraw-Hill, Inc., New York, NY, pp. 450–452.
Wu, K., 2003. Water regime change characteristics and sustainable development of irrigation areas diverted water from Lower Reach of the Huanghe River. Journal of Irrigation and Drainage 22 (1), 45–47 (in Chinese).
Xiao, J.F., Liu, Zh.D., Duan, A.W., Liu, Z.G., Li, X.D., 2006. Irrigation studies on effects of irrigation systems on the grain yield constituents and water use efficiency of winter wheat. Journal of Irrigation and Drainage 25 (2), 20–23 (in Chinese).
Yang, J.F., Li, B.Q., Liu, S.P., 2000. A large weighing lysimeter for evapotranspiration and soil water–groundwater exchange studies. Hydrological Processes 14 (10), 1887–1897.
Yang, J.F., Wan, S., Deng, W., Zhang, G., 2007. Water fluxes at a fluctuating water table and groundwater contributions to wheat water use in the lower Yellow River flood plain, China. Hydrological Processes 21 (6), 717–724.
Yang, Y.M., 2005. Calibration & Validation and Application of Cotton Simulation Model COTTON2K. PhD Dissertation, Graduate University of Chinese Academy of Sciences, Beijing, China (in Chinese).
Yu, J.J., 2002. High-efficiency Use of Agricultural Water Resources in the Irrigation Areas along the Lower Reaches of the Yellow River: A Case Study of Gaotang County. PhD Dissertation, Graduate University of Chinese Academy of Sciences, Beijing, China (in Chinese).
Zhang, S.Q., Zhou, X.P., Mu, Z.X., Shan, L., Liu, X.F., 2009. Effects of different irrigation patterns on root growth and water use efficiency of maize. Transactions of the CSAE 25 (10), 1–6 (in Chinese).
Zhang, X.Y., Du, J.D., Zheng, D.F., Feng, N.J., Zhang, Y.X., Liang, X.L., Ding, X.W., 2006. Studies on the relationship between yield and leaf area index and their dry matter accumulation dynamic on the different population. Chinese Agricultural Science Bulletin 22 (11), 161–163 (in Chinese).
Zhang, Y.Q., Mao, X.S., Sun, H.Y., Li, W.J., Yu, H.N., 2002. Effects of drought stress on chlorophyll fluorescence of winter wheat. Chinese Journal of Eco-agriculture 10 (4), 13–15 (in Chinese).
Zhu, Z.X., Zhang, J.C., 1991. Crop Water Stress and Drought. Henan Science and Technology Press, Zhengzhou, China.